Copyright Warning & Restrictions

The copyright law of the United States (Title 17, United States Code) governs the making of photocopies or other reproductions of copyrighted material.

Under certain conditions specified in the law, libraries and archives are authorized to furnish a photocopy or other reproduction. One of these specified conditions is that the photocopy or reproduction is not to be "used for any purpose other than private study, scholarship, or research." If a, user makes a request for, or later uses, a photocopy or reproduction for purposes in excess of "fair use" that user may be liable for copyright infringement,

This institution reserves the right to refuse to accept a copying order if, in its judgment, fulfillment of the order would involve violation of copyright law.

Please Note: The author retains the copyright while the New Jersey Institute of Technology reserves the right to distribute this thesis or dissertation

Printing note: If you do not wish to print this page, then select "Pages from: first page # to: last page #" on the print dialog screen

ABSTRACT

INVESTIGATION OF THE REACTION KINETICS OF HYDROGEN CHLORIDE WITH CALCIUM OXIDE BY FOURIER TRANSFORM-INFRARED SPECTROSCOPY

by
Maosheng Li

The kinetics of HCl reaction with CaO was investigated over the temperature range of 148 to 400 ^{o}C. A thin film of CaO was deposited on quartz wool and used as the sorbent. The HCl concentration was maintained uniformly in the closed system with a circulating pump in order to minimize the effects of the bulk mass transfer and pore diffusion. The HCl concentration was continuously monitored in a FT-IR cell and the HCl and H_2O spectra were collected automatically by GC software at 1.2 second intervals. In this way, fewer errors were introduced into the system. The results showed excellent agreement of the data with first order reaction kinetics with respect to HCl concentration. The activation energy of 7490 kJ/mol is slightly larger than reported by others and indicative of the real kinetics of HCl with CaO surfaces.

INVESTIGATION OF REACTION KINETICS OF HYDROGEN CHLORIDE WITH CALCIUM OXIDE BY FOURIER TRANSFORM-INFRARED SPECTROSCOPY

by
Maosheng Li

A Thesis
Submitted to the Faculty of
New Jersey Institute of Technology
in Partial Fulfillment of the Requirements for the Degree of
Master of Science in Environmental Science

Department of Chemical Engineering, Chemistry, and
Environmental Science

October 1993

APPROVAL PAGE

Investigation of The Reaction Kinetics of Hydrogen Chloride with Calcium Oxide by Fourier Transform-Infrared Spectroscopy

Maosheng Li

Dr. Henry Shaw, Thesis Advisor Professor of Chemical Engineering, NJIT	date
Dr. Barbara Kebbekus, Committee Member Associate Chairperson and Professor of Chemistry, NJIT	date
Dr. Robert B. Barat, Committee Member Assistant Professor of Chemical Engineering, NJIT	date

BIOGRAPHICAL SKETCH

Author: Maosheng Li

Degree: Master of Science in Environmental Science

Date: October 1993

Undergraduate and Graduate Education:

- Master of Science in Environmental Science,
  New Jersey Institute of Technology, Newark, NJ 1993
- Master of Science in Chemistry,
  East China University of Chemical Technology, China,
  1986
- Bachelor of Science in Chemistry,
  East China University of Chemical Technology, China,
  1983

Major: Environmental Science

Presentations and Publications:

Maosheng Li, Henry Shaw, Chen-lu Yang, G.C. San Agustin
Investigation of Kinetics of HCl Reaction with CaO by FT-IR."
Forth Annual MINI-TECH Student Conference. Stevens Institute of Technology, NJ, April 16, 1993

Maosheng Li, Linxian Shao, Xinrong Jin, "Preparation & Application of Thick Film Capillary Columns Immobilized by ^{60}Co Radiation,"
Chinese Journal of Chromatography (SePu), Oct., 1987

Maosheng Li, Linxian Shao, Xinrong Jin, "Investigation of Volatile Constituents of Grape Must and Grape Wine by GC/MS/DA."
Chinese Journal of Chromatography (SePu), Dec., 1987

This thesis is dedicated to

Dr. Henry Shaw

ACKNOWLEDGMENT

The author wishes to express her sincere gratitude to her supervisor, Professor Henry Shaw, for his guidance, friendship, and moral support through this research.

Special Thanks to Professor Barbara B. Kebbekus and Assistant Professor Robert B. Barat for serving as members of the committee.

Many thanks are due to Chen-lu Yang, a Ph.D candidate of Chemical Engineering and Gwen C.San Agustine, Chemist in Hazardous Substance Management Research Center for their timely and valuable assistance in experimental design and analytical techniques.

The author is grateful to the Hazardous Substance Management Research Center for providing FT-IR/GC and related facilities to carry this research work..

The author appreciates the help from Yogesh Ghandhi, Manager of the Chemistry stockroom for providing laboratory related facilities to carry out this research work.

Finally, a thanks to members of gas scrubbing and Catalytic Incineration Laboratory, including Chung-Der Chen, Tai-chiang Yu, Yi Wang for their help.

TABLE OF CONTENTS

Chapter **Page**

Chapter **Page**

List of Figures

List of Table

CHAPTER ONE

INTRODUCTION

The treatment of the acid gases from incinerator effluents is receiving much attention by federal, state and local regulators, as well as from the general public. Environmentalists and the industry agree that polyvinylchloride plastics (PVC) is the major contributor to hydrogen chloride (HCl) in incinerator flue gases [1]. The rest of the hydrogen chloride is produced from the destruction of toxic halogenated organic wastes, such as pesticides, various chlorinated solvents, waste polychlorinated biphenyls (PCB) from industrial use, and also inorganic chlorides such as sodium chloride (common salt), paper products, etc. The Resource Conservation and Recovery Act (RCRA) regulations require 99 % removal of hydrogen chloride or HCl emission concentration below 180 mg/dsm^3 (milligram/dry standard cubic meter)) at 7 % O_2 in the operation of an incinerator system. It was reported [2] that HCl levels were well beyond the upper limit of the concentration prescribed by air pollution control regulation. Therefore, industrial and municipal treatment facilities need to consider ways of reducing emissions of HCl to acceptable values.

1.1 Methods of Hydrogen Chloride Removal

The processes that can be used for the control of HCl emissions when chlorinated compounds are incinerated can be classified as "wet" or "dry" processes. Removal of HCl gas would take place during or after the incineration process.

The wet methods employ a slurry or solution of some suitable absorbent in conventional gas-liquid contacting devices. The conventional Wellman-Lord wet process incorporates two stage gas-liquid contacting devices. In the first stage, usually referred to as the pre-scrubber, the hot gas is cooled to about 60 ^{o}C and saturated with water where HCl in hot flue gas is neutralized by alkaline solution, and then go second stage passing to the main sulfur dioxide absorber.

Wet processes remove HCl gas from hot flue gas by absorption, but they have two disadvantages. This approach invariably transforms an air pollution problem into a water pollution problem. Furthermore, these processes waste energy because they seldom recover the heat content in the flue gases from the incinerators. The flue gas temperature range can vary from about 150 ^{o}C to 1000 ^{o}C depending on internal heat recovery methods. In a special case for the EPA SITE program where the hot flue gas temperature can be over 500 ^{o}C, an expensive flue gas-to-air heat exchange would be needed to cool the flue gases in order to clean the gases by alkaline aqueous scrubbing prior to emitting it to the atmosphere. Furthermore, the HCl containing flue gas can be extremely corrosive to such heat exchangers.

In dry processes, solid high temperature sorbents would be used to remove acid gases. In this case, the flue gas can be used to do work since the HCl is removed at high temperature without fear of corroding the energy recovery devices. In his 1992 M.S. thesis at NJIT, Qian Lao [3] showed that calcium-based compounds adsorbed HCl quantitatively up to 1000 K. He studied the effect of various particle sizes to determine the trade-off between adsorption effectiveness and pressure drop. Over 80% of the calcium content of the sorbent CaCO3 was utilized for particles

under 40 um. Therefore, the reaction of Ca-based sorbents with HCl is of interest for control of acid gas emissions from incineration processes.

1.2 Objective and Significance of the Research

The objective of this thesis is to determine the kinetics of HCl reaction with CaO at the conditions which minimize the effects of the bulk mass transfer and pore diffusion. Since Lao did his research with various particle sizes, it wasn't clear whether the measurements he made were partly due to surface diffusion or represented true gas-solid chemical kinetics. The secondary objective was to develop methodology for the measurement of real-time gas-solid reaction kinetics using Fourier transform-infrared spectroscopy (FT-IR) and associated GC-32 software.

CHAPTER TWO

BACKGROUND

The reaction of Ca-based sorbents with HCl is a non-catalytic gas-solid reaction. The following calcium based reactions can be used to remove HCl, and the standard heats of reaction (ΔH°) are given at 298 K:

$$CaCO_3(s) + 2HCl(g) \rightarrow CaCl_2(s) + CO_2(g) + H_2O(g) \quad (2\text{-}1)$$

$$\Delta H^\circ = -7{,}843 \text{ cal}$$

$$Ca(OH)_2(s) + 2\,HCl(g) \rightarrow CaCl_2(s) + 2\,H_2O(g) \quad (2\text{-}2)$$

$$\Delta H^\circ = -24{,}240 \text{ cal}$$

$$CaO(s) + 2\,HCl\,(g) \rightarrow CaCl_2(s) + H_2O(g) \quad (2\text{-}3)$$

$$\Delta H^\circ = -50{,}342 \text{ cal}$$

At high temperatures, $CaCO_3$ and $Ca(OH)_2$ decompose:

$$CaCO_3(s) \Longleftrightarrow CaO(s) + CO_2(g) \quad (2\text{-}4)$$

$$\Delta H^\circ = 42{,}499 \text{ cal/mol}$$

$$Ca(OH)_2(s) \Longleftrightarrow CaO(s) + H_2O(g) \quad (2\text{-}5)$$

$$\Delta H^\circ = 26{,}105 \text{ cal/mol}$$

The flue gas from an incinerator can be very hot if no heat recovery is practiced. The range of temperatures in this case is from about 500 to 1000 $^\circ$C. Thermal decomposition of calcium hydroxide [$Ca(OH)_2$] and calcium carbonate ($CaCO_3$) due to flue gas in this temperature range results in the loss of H_2O and CO_2, respectively, and formation of CaO. Therefore, HCl reaction with CaO was investigated in this thesis.

2.1 Literature Review

Various types of Ca-based systems for HCl removal are discussed in the literature and a few experimental results were reported, covering a wide range of operating conditions and systems[4, 5, 6, 7, 8]. Numerous waste combustion facilities use some type of sorbent injection for acid gas control, but very little fundamental kinetic information has been published to assist design efforts and optimize performance.

Until now, only four publications was found that elucidate some of the important parameters regarding the Ca/HCl reaction.

Kaalson et al., [4] measured a first-order rate law with HCl concentration when running breakthrough analysis with HCl and $Ca(OH)_2$ from 150 to 400 ^oC.

Walters and Daoudi [5] found the reaction of CaO and HCl to be first order with respect to gas-phase HCl concentration (0.5-5.0 mol%). They determined that the intrinsic chemical reaction rate constant was governed by an Arrhenius expression with an activation energy of 20.9 kJ/mol (5 kcal/mol) between temperatures of 500 and 650 ^oC.

Weinell et al., [6] studied the direct reaction of $Ca(OH)_2$ with HCl between 60 and 1000 ^oC, finding maximum sorption in the 500-600 ^oC range. The sorptive capacity was found to be independent of particle size over the range 2.12 to 20.5 um, and only minor effects of initial surface area (range 8-20 m^2/g) were observed. Reaction kinetics were controlled by gas diffusion through the solid product, governed by a diffusivity with an activation energy of 10-15 kJ/mol (2.4-3.6 kcal/mol).

Gullett et al., [7] investigated the kinetics of the reaction between CaO and HCl under conditions that minimized bulk mass transfer and pore diffusion limitations. Reactivity data from 0.2 to 1 second exposure

to 5000 ppm HCl in a fixed bed reactor were obtained and modeled using a shrinking core model in diffusion and chemical reaction control either independently or in combination. Between temperatures of 150 and 350 ^{o}C, the reaction is controlled by gaseous diffusion through the developing product layer. The apparent activation energy is about 28.1 kJ/mol (6.7 kcal/mol), and the reaction is first order with respect to HCl concentration. Reactivity was found to be a minor function of the measured particle size and surface area.

2.2 Review of Gas-Solid Reaction Model

A conceptual model or picture is necessary to give a reasonable illustration of the phenomenological results and to analyze quantitatively a single particle reaction system. The model described in this section followed the treatment that Daoudi [8] presented in his doctoral dissertation. A group of equations may then be set up to describe the system and allow a quantitative relationship to be established among system parameters. The criterion for a good model is that it is the closest representation of the actual phenomenon which can be treated without undue mathematical complexities.

The steps that are to be considered in the conceptual model and which will determine the global, or overall, rate of reaction for a solid-gas system consist of the following [9, 10]:

1. Transport of the gas reactants from the bulk gas to the gas-solid interface.
2. Intraparticle transport of gas reactants through the porous solid or product layer.
3. Adsorption of the gas reactants at the solid reactant surface.

4. Chemical reaction between gas and solid reactants

5. Desorption of the gas products from the solid reaction surface.

6. Transport of gas products from the reaction surface through the porous solid medium.

7. Transport of gas products from the gas-solid interface into the bulk gas stream.

Finally, another parameter which is seldom considered in gas solid reaction modelling, but nevertheless is important, and affects gas-solid kinetics is:

8. Structural changes such as size, shape, sintering, crystal structure, etc. due to chemical reaction. Changes in size, due to different densities of solid reactant and product are always included in modelling efforts.

For heterogeneous reactions the first seven steps occur consecutively and may be regarded as resistances in series. In developing the mathematical model one would consider the various steps as they occur over a wide range of conditions. This is due to the fact that in practical systems, one single rate determining step is a limiting case, and therefore, a combination of these steps is usually rate controlling. However, a rigorous mathematical treatment of a model accounting for all events is very difficult. Therefore certain assumptions have to be made in order to develop a more detailed understanding of the rate controlling step(s).

a. Usually steps 3, 4 and 5 are combined and the overall surface effects are treated as an n order rate equation in the model [9]. Alternatively, steps 3 and 5 may not even be visualized

as part of the sequences which determine the global rate [11].

b. The resistance offered by steps 6 and 7 may be neglected in the case of the irreversible reactions or where no gaseous products are formed.

With the above assumptions, the only remaining resistances are gas-phase mass transfer resistance, the internal diffusion resistance in the solid, and the intrinsic reaction resistance.

For a gas-solid reaction

$$aA\,(g) + bB\,(s) \longrightarrow eE\,(g) + fF\,(s)$$

Three models, shrinking core model, volume reaction model, grain model[10], have been widely used in the literature for reactions similar to the ones described above. Choice of the most appropriate ones is based on the initial form of the solid reactant and the changes that occur with reaction.

2.2.1 Shrinking Core Model[10]

In shrinking core model, also called unreacted core model, the reaction will occur at its outer surface of nonporous reactant, B. This surface recedes with extent of reaction, as shown in figure 2.1a. As reaction occurs, a layer of product, F, builds up around the unreacted core of reactant, B. A porous particle might also behave in this way if the resistance to reaction is much less than the resistance to diffusion of fluid reactant in the pores of the particle. The key factor in this model is

that the reaction always occurs at a surface boundary, that is , at the interface between unreacted core and surrounding solid product.

2.2.2 Volume Reaction Model[10]

Suppose the solid reactant is so porous that the gas reactant, A, can reach all parts of the solid reactant, B, without pore diffusion resistance; this is depicted in figure 2-1b. Now the rate per particle will vary as the surface of solid reactant, B, changes with time and the layer of solid product, F, accumulates. The key factor here is that the concentration of reactant within the particles. Therefore, the volume reaction model is sometimes referred to as the "homogeneous model", the "continuous reaction model", and the "dispersed-solid model".

2.2.3 Grain Model[10]

In this model, the solid pellet reactant, B, is visualized as consisting of a number of very dense particles or grains. This is shown in figure 2.1c. The pores surrounding the particles are supposed to be small enough that concentration of gas reactant, A, decreases significantly toward the center of the pellet.

The grain model is particularly useful for the case where a solid pellet is formed by compaction of particles of very fine size.

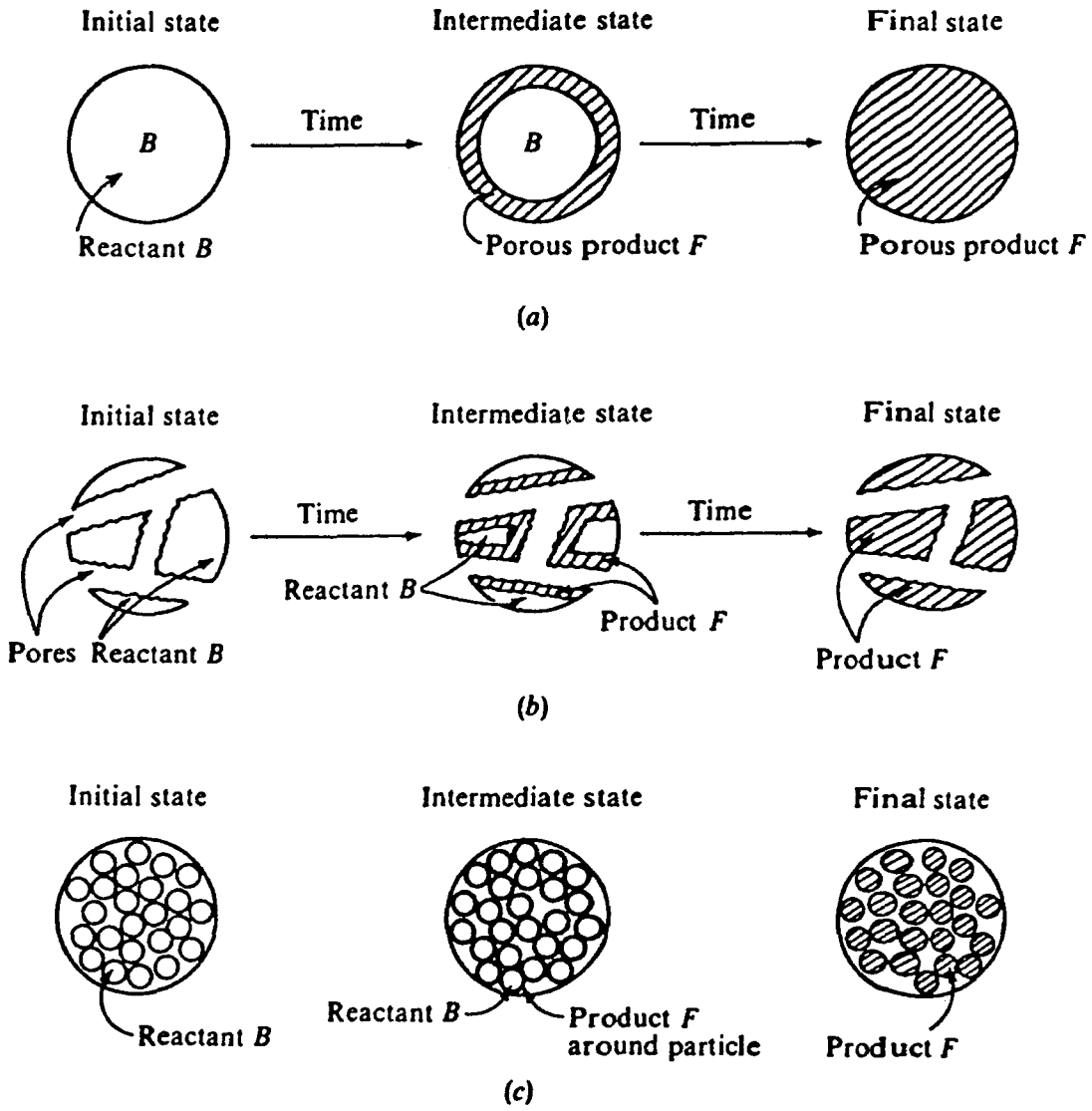

Figure 2.1 Models for gas-solid noncatalytic reactions of the type aA (g) + b B (s) —> eE (g) + fF (s): (a) shrinking-core model, (b) volume reaction model, (c) grain model[9]

CHAPTER THREE

EXPERIMENTAL

In this chapter, the equipments, experimental apparatus and methods, and materials used for the investigation of the kinetics of CaO with HCl will be discussed.

3.1 Equipment

A detailed description of the equipment used to conduct the research presented in this thesis is provided in this section.

3.1.1 Pump

The pump is used to circulate a gaseous mixture of hydrogen chloride and nitrogen in the reaction system during the progress of the HCl reaction with CaO to minimize external mass transfer and pore diffusion effects.

A series 7591 Masterflex Pump Drive System (including Pump Drive, Controller, Controller and Motor Cables) and Model 7529-10 Masterflex Industrial/Process (I/P) Easy-load Pump Head (Cole-Parmer Instrument Co.) was used to circulate the gases through the detector cell of the FT-IR instrument. The tubing for the pumping application was Pharmed (size 81). Although the experimental apparatus could tolerate a maximum circulating rate 13.2 liter per minute, the average circulation rate was 12 liter/min.

3.1.2 Chloride Selective Electrode and pH Meter

An Orion Model 96-17B combination chloride ion selective electrode (CSE) was used to check the HCl concentration from the gas cylinder and also to monitor the appearance of HCl after breakthrough. This was done by bubbling a known amount of the gas mixture through a $NaNO_3$ solution and using the precalibrated CSE to measure the aqueous chloride ion concentration. The chloride electrode measures free chloride ions in aqueous solutions.

A Jenco model 6071 microcomputer based Bench pH meter, was used to read the output from the chloride selective electrode. A built-in computer stores, calculates and compensates all the temperature characteristics of the pH electrode, buffer solution and electrode slope deviation.

3.1.3 FT-IR Spectrometer

FT-IR spectrometer (BIO-RAD Laboratories, Inc., Digilab Division) was employed in conjunction with the 3200 Data System and GC-32 software (see Appendix 2 for detail). The GC-32 software is designed for kinetic studies. Kinetic studies measure spectroscopic changes as a function of time, and involve collecting a series of spectra through an entire experiment at a rate that resolves the changes of interest. The species whose spectra can be obtained in this way could be reaction intermediates or elution fractions. The primary kinetic application of GC-32 software is capillary column GC/IR. For this reason, the GC-32 Operation 's Manual is structured for capillary GC/IR work, and the discussion, terminology and parameter set values follow GC/IR usage. Therefore, in order to make GC-32 fit kinetic studies for HCl reaction

with CaO, we changed the fixed parameters of GC/IR usage. The reactor took the position of the capillary column. IR beam was switched to the main IR window.

The reaction of HCl with CaO can be measured by monitoring the consumption of HCl which is directly proportional to the overall fractional conversion of HCl gas for a first order reaction. Thus GC-32 software was used to continuously process data for measurements of HCl spectroscopic changes following the progress of the reaction and automatically collect and store the spectra at 1.2-s intervals

3.1.4 Experimental Apparatus

Figure 3.1 is the schematic diagram of the experimental apparatus. It can be divided into three modes of operation (Figures 3.2, 3.3, and 3.4) and two cycles (Figure 3.1) by switching the valves.

The IR cell, modified with ZnSe windows, was kept in the path of IR rays inside the FT-IR spectrometer. This arrangement helped us to heat the sample externally to any desired temperature.

The pump was used to recirculate the gases in the reaction system to minimize the effects of mass transfer and pore diffusion.

The reaction was carried out in the quartz tubular reactor with 1 inch I.D. and 15 inch length. A quartz frittered disc was used to contain CaO adsorbent on quartz wool in the center of reactor. The reactor was put in a horizontal tubular resistance heated furnace. The temperature of reactor was controlled by adjusting a furnace temperature controller and measured with a 0.16 cm chromel-alumel (K-type) thermocouple which was inserted into the center of CaO on quartz wool reactant. The

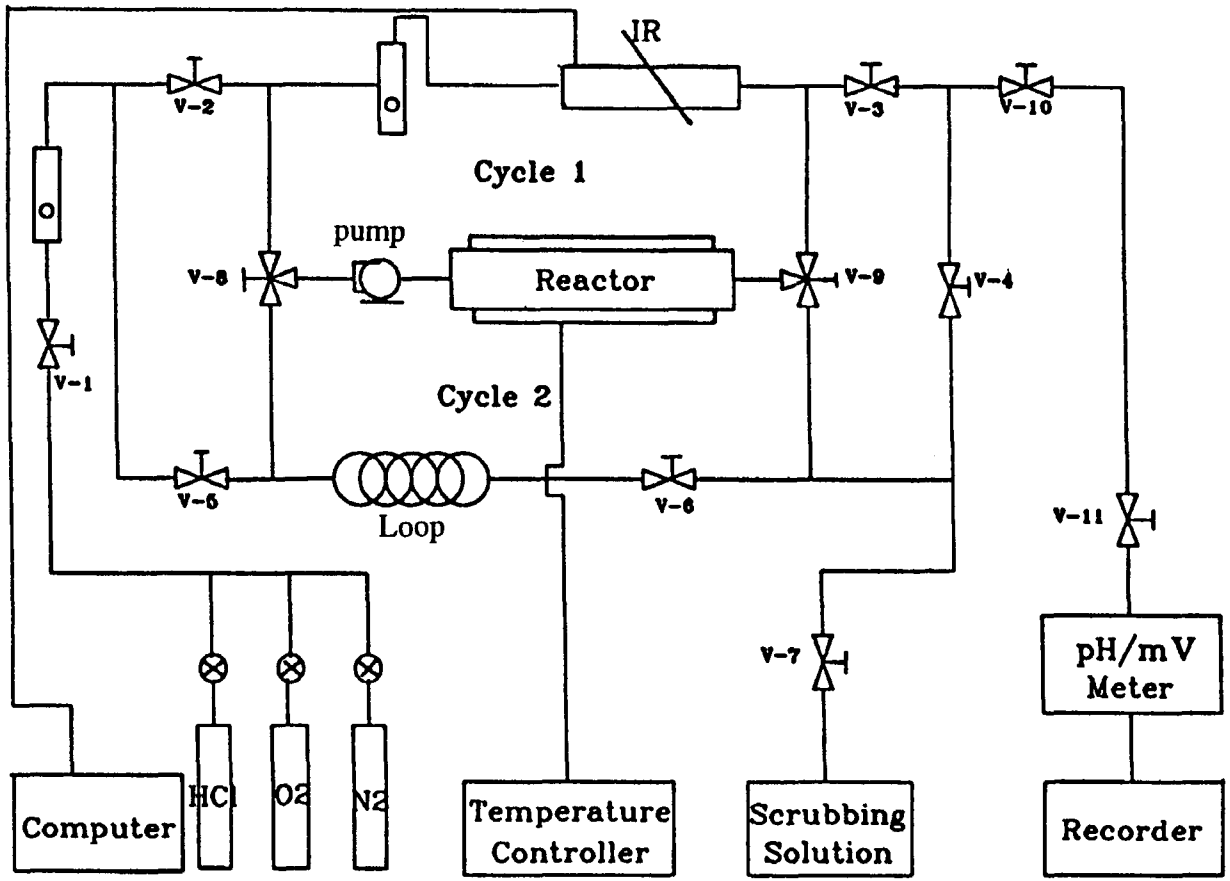

Figure 3.1 Schematic diagram of reaction system

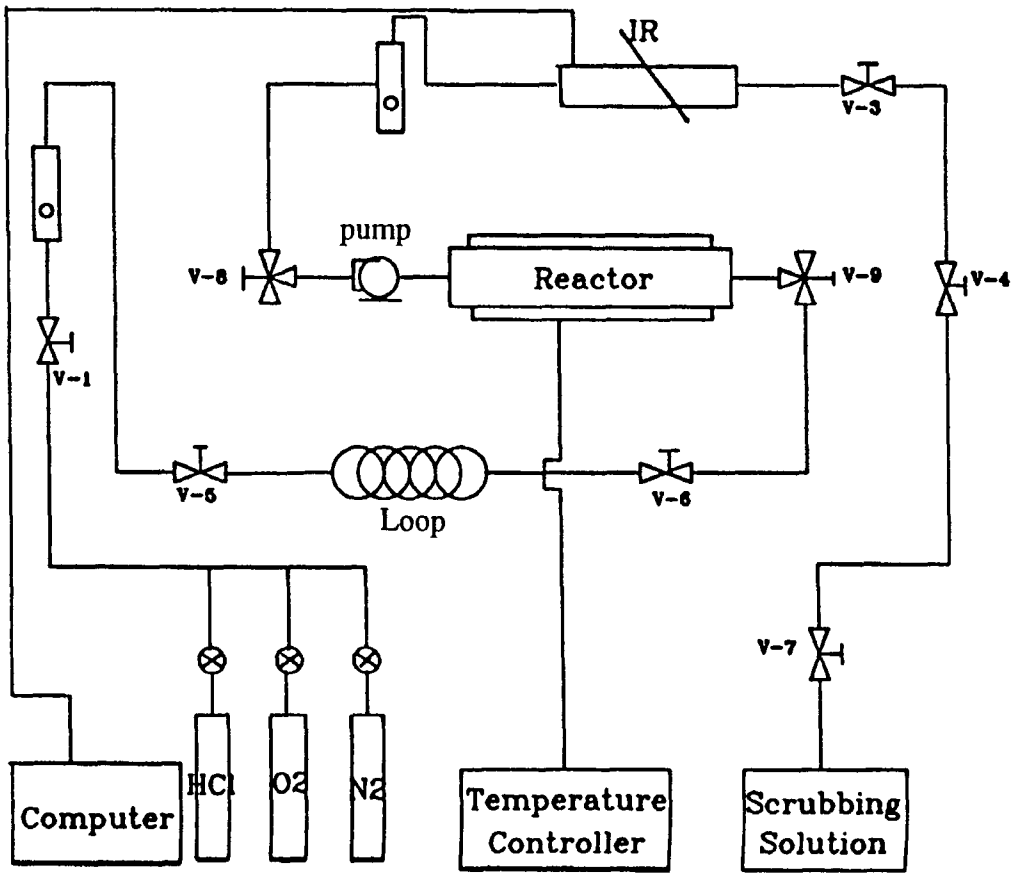

Figure 3.2 Operating mode 1

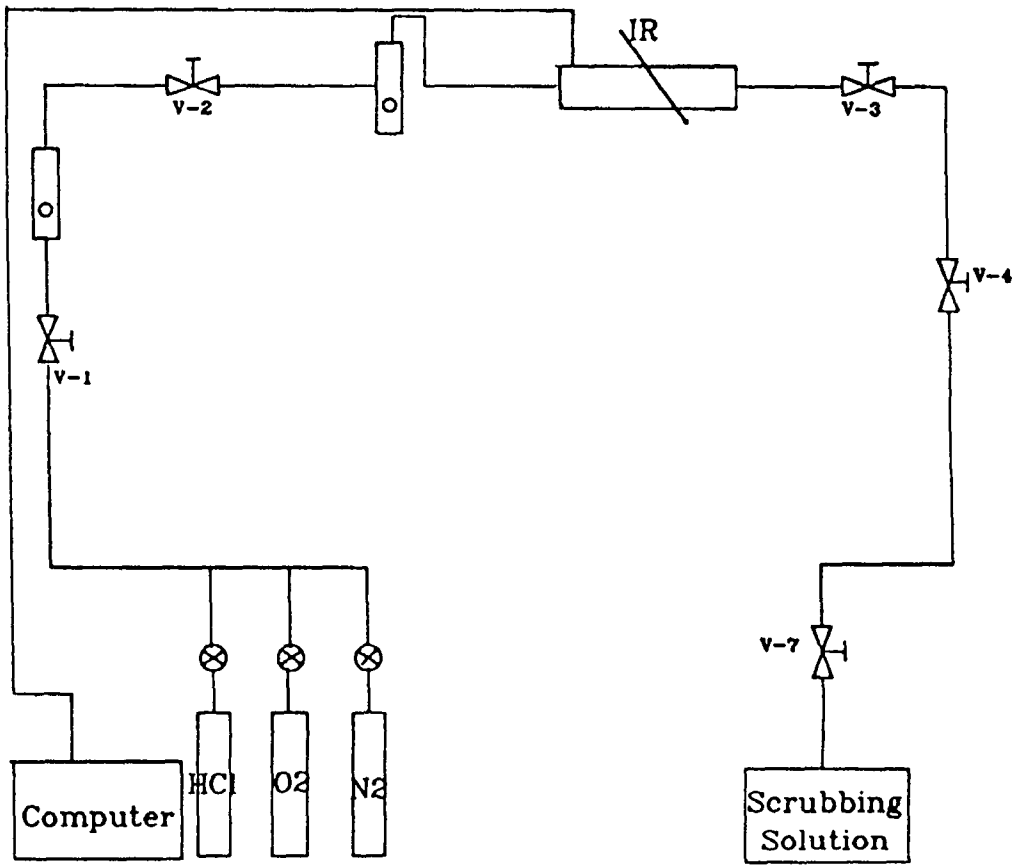

Figure 3.3 Operating mode 2

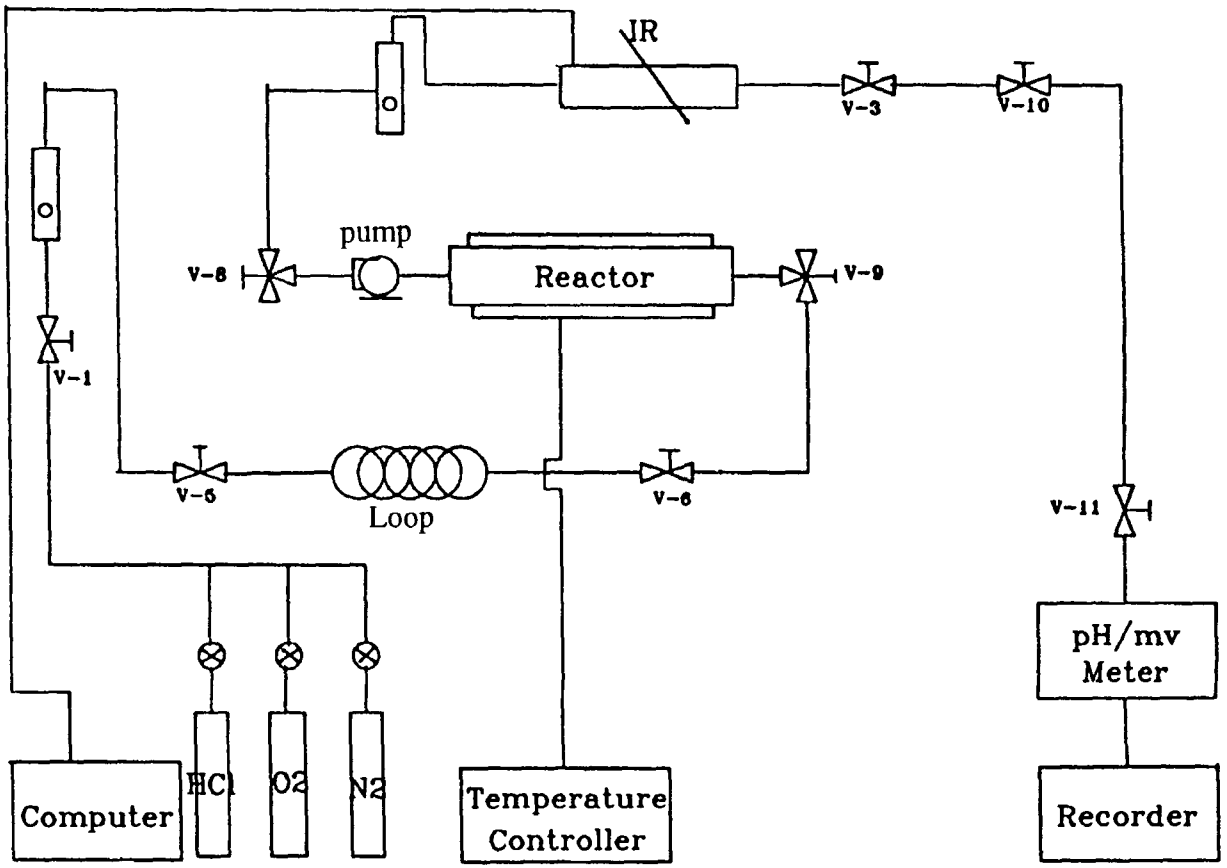

Figure 3.4 Operating mode 3

difference among the furnace set temperature, measured furnace temperature, measured quartz wool reactor temperature is shown on figure 3.5.

The experimental apparatus is used to measure four key parameters:

1. Preparation and quantitative amount of CaO deposited on quartz wool using operating mode 1 (Figure 3.2) and operating mode 2 (Figure 3.3)
2. Analysis of the initial concentration of HCl gas from the gas cylinder using operating mode 2 (Figure 3.3)
3. Analysis of the monitoring of the reaction progress of HCl with CaO using operating mode 1 (Figure 3.2), operating 2 (Figure 3.3), cycle 1 and cycle 2 (figure 3.1)
4. Breakthrough analysis of CaO reaction capacity using operating mode 3 (Figure 3.4)

3.2 Determination of HCl Concentration

The measurement of HCl concentration from gas cylinder consists of sampling, analysis and preparation of a calibration curve of chloride ion concentration, which is discussed in this section.

3.2.1 Sampling and Analysis

HCl gas passed operating mode 2 (Figure 3.3) through 125 ml of distilled water which contained 2 ml of 5N $NaNO_3$ at 237 liter/min for 2 minutes and was absorbed. The scrubbing solution was analyzed by chloride selective electrode.

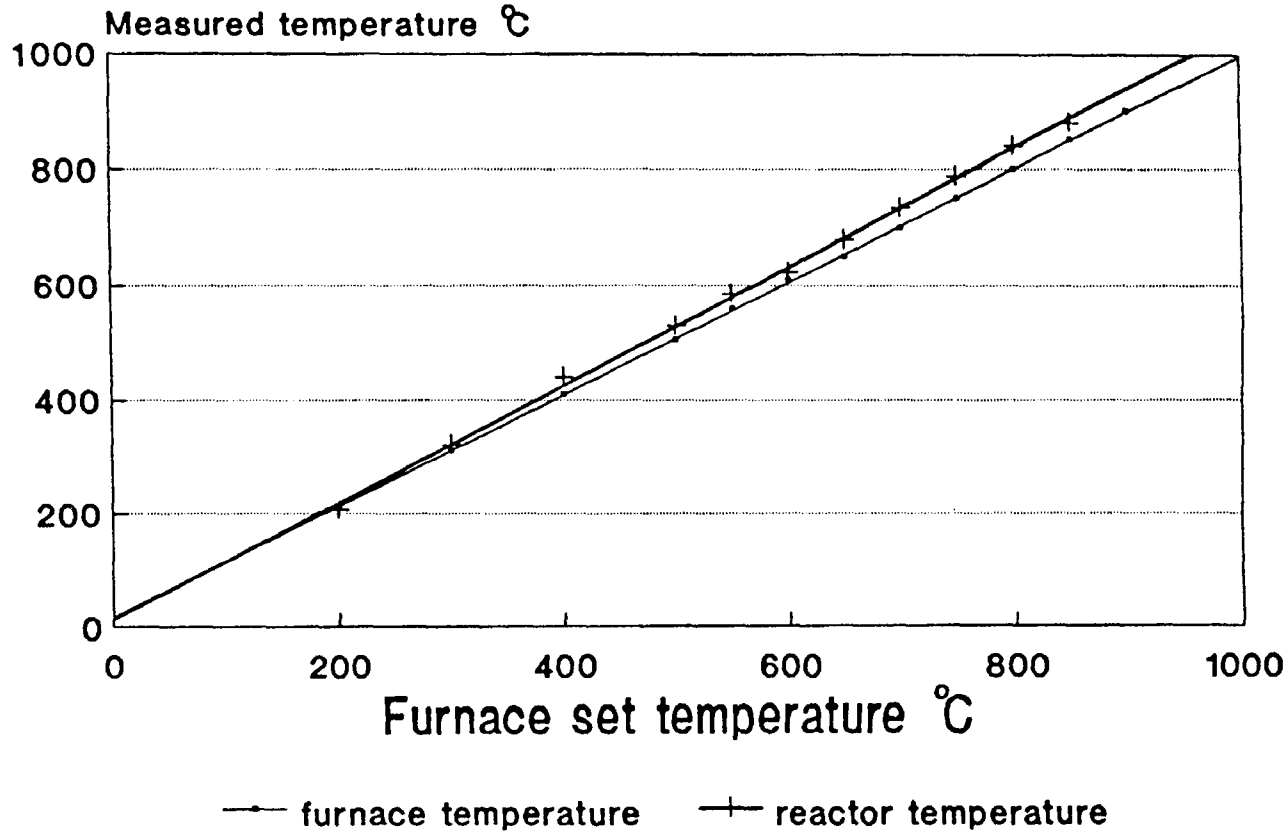

Figure 3.5 Relationship of furnace set temperature , furnace temperature , reactor temperature

3.2.2 Calibration Curve of Chloride Ions

A chloride ion calibration curve was obtained from diluted standard solutions, containing 2 x 10^{-4}, 4 x 10^{-4}, 6 x 10^{-4} and 8 x 10^{-4} M NaCl. Measure each standard by CSE. The potential of each standard concentration was plotted against the concentration.

If the potential of the scrubbing solution was out of the standard range, it was diluted and then measured.

3.3 Preparation of CaO Adsorbents

The method for depositing and measuring the quantity of CaO on quartz wool is described in this section.

3.3.1 Depositing $Ca(NO_3)_2$ on Quartz Wool

Approximately 0.5 g quartz wool was weighed and immersed into 0.1 M $Ca(NO_3)_2$ solution. The wet quartz wool was removed from the solution and spread on a platter. The quartz wool with platter was placed in an oven to dry at about 150 ^{o}C. In this way, $Ca(NO_3)_2$ is assumed to be uniformly deposited on the quartz wool.

3.3.2 Conversion of $Ca(NO_3)_2$ to CaO

After soaking the solution of $Ca(NO_3)_2$ on quartz wool, the quartz wool is placed in the reactor. The valves (Figure 3.1) are positioned to allow O_2 flow to operating mode 1 (Figure 3.2). Reactor temperature is maintained at 400 ^{o}C for about 1 hour to remove H_2O. The valves to the reactor are then closed and the temperature is increased to 700 ^{o}C and kept for about 3 hours to quantitatively convert $Ca(NO_3)_2$ to CaO. The reactor is cooled for measurement of NO_2 from the conversion of $Ca(NO_3)_2$ to CaO.

3.3.3 Determination of NO_2 from the Conversion of $Ca(NO_3)_2$ to CaO

Based on equation (3-1)

$$Ca(NO_3)_2 \text{ ----> } CaO + 2\ NO_2 + 1/2\ O_2 \qquad (3\text{-}1)$$

one can see that 2 moles of NO_2 are produced for every of CaO produced. Therefore, in order to measure how much CaO was deposited on the quartz wool, we determined the amount of NO_2 given off from the decomposition of $Ca(NO_3)_2$. The IR cell, in conjunction with the GC-32 software, allow a convenient and accurate measurement of NO_2. IR scan started from 4000 to 700 cm^{-1}

3.3.3.1 Procedure for Measurement of NO_2 from the Conversion

There are two steps in the measurement of NO_2 from the conversion of $Ca(NO_3)_2$ to CaO.

1. Background Measurements—the valves were positioned to allow O_2 to pass through operating mode 2. The GC-32 program is used to collect O_2 IR background data.
2. "Injection" of NO_2—the valves were quickly switched to allow O_2 to flow to operating mode 1 (Figure 3.2). O_2 carried NO_2 from the reactor to the IR cell. Here, switching valves are operated just like a GC injection valve. The GC-32 software allows the FT-IR to produce a NO_2 peak in the gas chromatogram (see Appendix 2). The area of peak is used to calculate the amount of NO_2 from the conversion of $Ca(NO_3)_2$ to CaO.

3.3.3.2 Calibration Curve of NO_2

A half percent of NO_2 in nitrogen was used as standard calibration gas. There are two steps to generate a NO_2 calibration curve.

1. The valves were positioned to allow N_2 to pass through operating mode 2 (Figure 3.3) at flow rate 438 ml/min. The GC-32 program signals to start data collection.
2. Inject 219, 438, 657, 876 ml of 0.5 % NO_2 by controlling the flow rate and time, separately into operating mode 2 (Figure 3.3). Each volume of NO_2 is injected three times. The calibration curve was prepared by plotting the volume of NO_2 injected into operating mode 2 vs. the peak areas.

3.4 Procedure for the Kinetics of HCl with CaO

After the measurement of NO_2, the kinetics of HCl reaction with CaO were measured by opening in operating mode 1 (Figure 3.2), operating mode 2 (Figure 3.3), cycle 1 and cycle 2 (Figure 3.1). The following reaction temperatures were used 148, 175, 203, 248, 275, 300, 330, 350, 400 ^{o}C. There are five steps in the experimental procedure.

1. Purge and Collect GC/IR Background—The valves are positioned to allow nitrogen flow to operating mode 1 (Figure 3.2), and reactor temperature is kept over 500 ^{o}C to remove possible contaminants. Maintain purge until the baseline of chromatogram became stable.
2. Equilibrate Reactor Temperature—The valves were switched to allow pump to recirculate nitrogen in cycle 2 (Figure 3.1) at a flow rate of 12.5 liter/min. The high recirculating rate makes the reactor temperature decrease quickly to a steady

state point which can be adjusted to the desired reaction temperature by increasing or decreasing the initial reactor temperature.

3. Obtain Initial Concentration of HCl—While equilibrating the reactor temperature, switch the valves to allow 4.9 % HCl gas to operating mode 2 (Figure 3.3). After the absorbance of the HCl becomes stable, close valve 2 and valve 3 in order to measure the initial reaction concentration of HCl. The initial HCl concentration is calculated by multiplying HCl concentration in gas cylinder by the dilution coefficient. When the valves were switched to allow the pump to recirculate the gases in cycle 1 (Figure 3.1), the HCl concentration was diluted by nitrogen gas.

4. HCl reaction with CaO—The valve are then quickly switched to allow the pump to recirculate HCl gas in cycle 1 (Figure 3.1). The HCl reaction with CaO is carried out in the reactor at the desired temperature.

5. Analysis—A series of HCl IR spectra at the desired reaction time interval are obtained after the GC collection by defining peak and scanning peak in the mode of Peak Edit. The peak at 2843 nm was used to investigate the kinetics of HCl with CaO.

3.5 Materials

HCl gas: 4.9 % HCl gas in N_2

N_2 gas: 99.99 %

O_2 gas: 99.9 %

NO_2 gas: 0.5 % in N_2

All gases above were supplied by Matheson Gas company.

Quartz wool: 99.8-99.9 % SiO_2 (Alltech Associates, Inc.)

$Ca(NO_3)_2$ H_2O: Analytical reagent (Mallinckrodt Chemical Works)

CHAPTER FOUR

RESULTS AND DISCUSSION

Nine experiments were done at constant temperature to investigate the kinetics of the reaction of HCl with CaO. Their results are presented and discussed in this chapter.

4.1 Analysis of HCl Gas

The concentration of HCl gas from compressed gas cylinder may change with time. In order to check the concentration of HCl gas, a chloride selective electrode (CSE) was employed to determine chloride ions. Figure 4.1 presents a calibration curve of chloride ion concentration with electrical potential.

4.1.1 Effect of pH on Chloride Ion Potential

The standard solutions were prepared with NaCl crystals. The pH of the scrubbing solution is lower than that of the standard solutions. Figure 4.2 shows that at lower pH values, the same concentration of chloride ions has a higher electrical potential. In order to overcome pH interference, 2 ml of ionic strength adjustor, 5 M $NaNO_3$ was added to all chloride standard solutions and scrubbing solutions so that the background ionic strength is high enough to be constant relative to variable concentrations of chloride ion and thus, eliminate background pH effects. Figure 4.3 shows that the responses of the chloride potential for the same chloride concentrations are almost same at different pH values, when an ionic strength adjustor is added to the chloride solution.

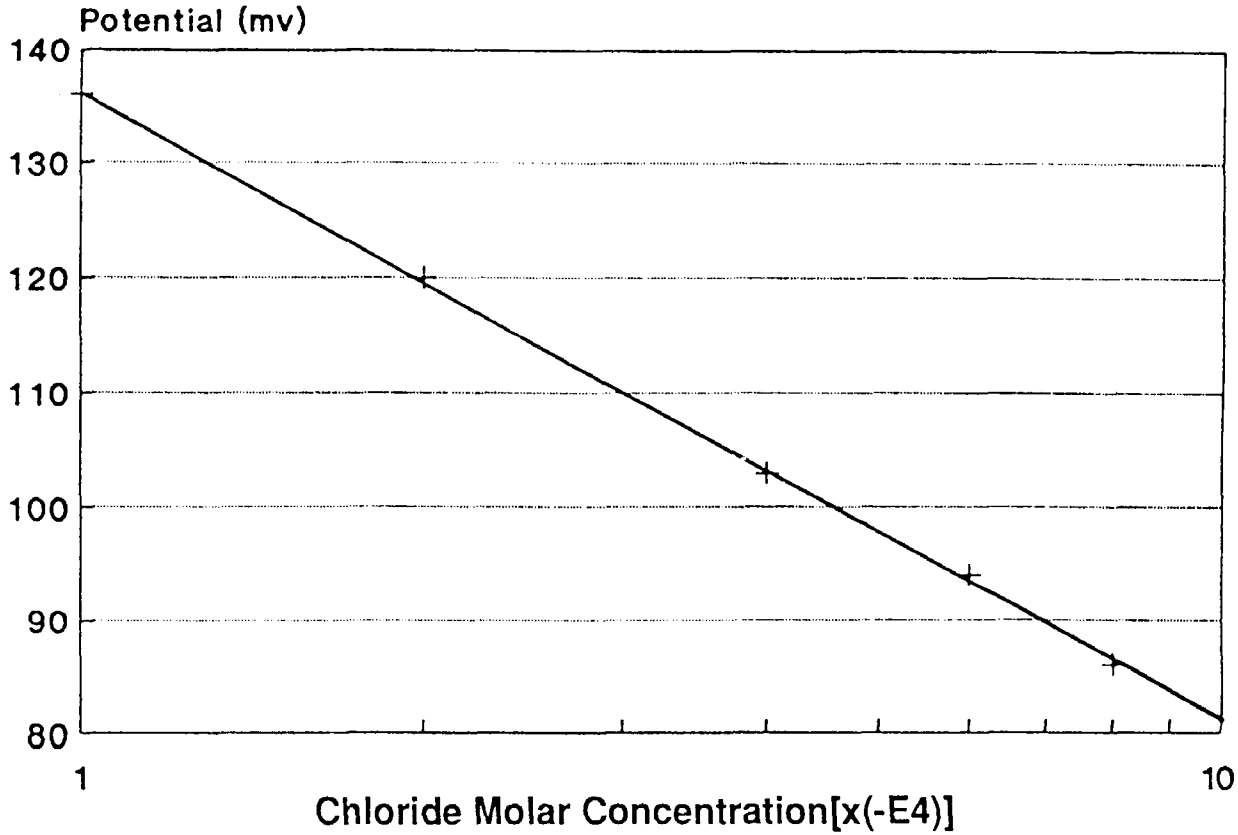

Figure 4.1 Calibration curve of chloride ions

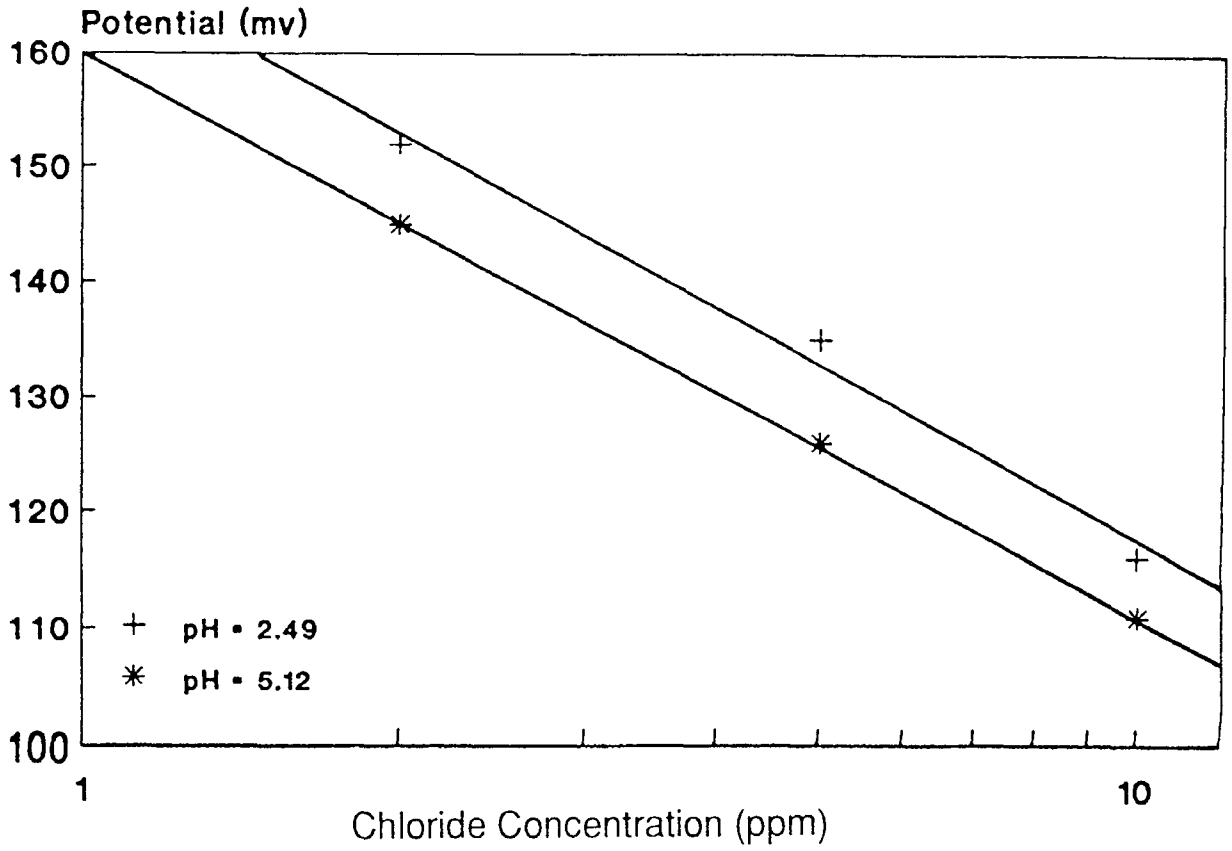

Figure 4.2 pH effect on chloride ionic electrode potential

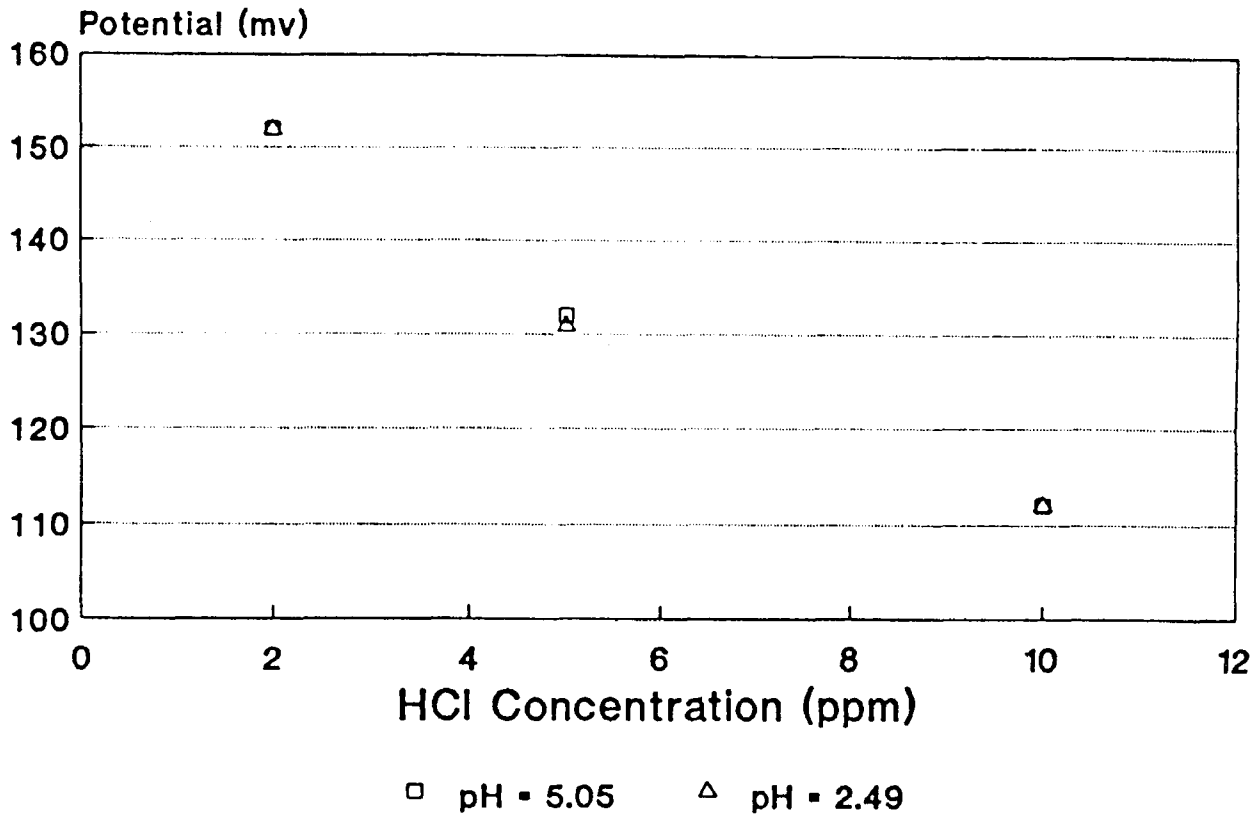

Figure 4.3 Effect of ionic strength adjustor in removing the pH effect bias in measuring HCl concentration

4.1.2 Concentration of HCl Gas from the Compressed Gas Cylinder

The test results for determining concentration of HCl gas from a compressed gas cylinder show that the concentration is a little bit different from the concentration, 4.9 % on the label based on mass spectroscopy when the cylinder was shipped. The change of HCL concentration is from 4.8 to 5.2 %. Therefore, the concentration of HCl gas should be checked before sorbent breakthrough analysis.

4.1.3 Effect of Temperature on Chloride Ionic Potential

In addition, during the breakthrough analysis, the gas from the reactor is hot and heats the scrubbing solutions to higher temperatures than those of the standard solutions. Since electrode potentials are affected by changes in temperature, the temperature of scrubbing solution and standard solution should be kept within $\pm$ 0.1 ^{o}C of each other.

4.2 Analysis of CaO Reactant

The methods used to ascertain how much CaO is collected on the quartz wool are described in this section.

4.2.1 Effect of Concentration of $Ca(NO_3)_2$ Solution on the Dispersion of CaO on Quartz Wool

When R. Gopalakrishnan [11] studied the kinetics of SO_2 with CaO, 5.3 gram of $Ca(NO_3)_2$ was dissolved into dilute HNO_3 to form $Ca(NO_3)_2$ solution and all the $Ca(NO_3)_2$ was dispersed on a known amount of quartz wool (exactly twice the amount of CaO). In our research, CaO reactants were prepared in the same way as R.Gopalakrishnan presented in his paper. The test results showed that CaO cannot be uniformly

dispersed on quartz wool. A different size of $Ca(NO_3)_2$ particles was formed on the surface of quartz wool. Also it took a relatively long time to convert $Ca(NO_3)_2$ particles to CaO. Therefore, we investigated how CaO can be uniformly deposited on quartz wool. The tests were carried out by putting 1 gram quartz wool into different concentration of $Ca(NO_3)_2$ solution (range from 5 M to 0.1 M $Ca(NO_3)_2$. The results showed that it is easier to disperse $Ca(NO_3)_2$ uniformly on quartz wool at lower concentration of $Ca(NO_3)_2$. It was found that 0.1 M $Ca(NO_3)_2$ solution gave excellent dispersion of CaO on quartz wool, and also sufficient amount of CaO on quartz wool for kinetic studies. In this way, CaO was deposited on quartz wool in a very thin film. It largely minimized potential interparticle diffusion.

4.2.2 Analysis of NO_2

FT-IR and GC software were used to determine how much NO_2 was produced from the conversion of $Ca(NO_3)_2$

4.2.2.1 Results

Figure 4.4 is the chromatogram from GC data collection. In order to check whether the peak represents only NO_2, we use IR to scan the peak and found that its spectrum was consistent with the spectrum (Figure 4.5) of 0.5 % NO_2 in N_2. The area of peak was used to calculate the amount of NO_2 from the conversion of $Ca(NO_3)_2$ to CaO.

According to stoichiometry of the reaction

$Ca(NO_3)_2$ ----> CaO + 1/2 O_2 + 2 NO_2

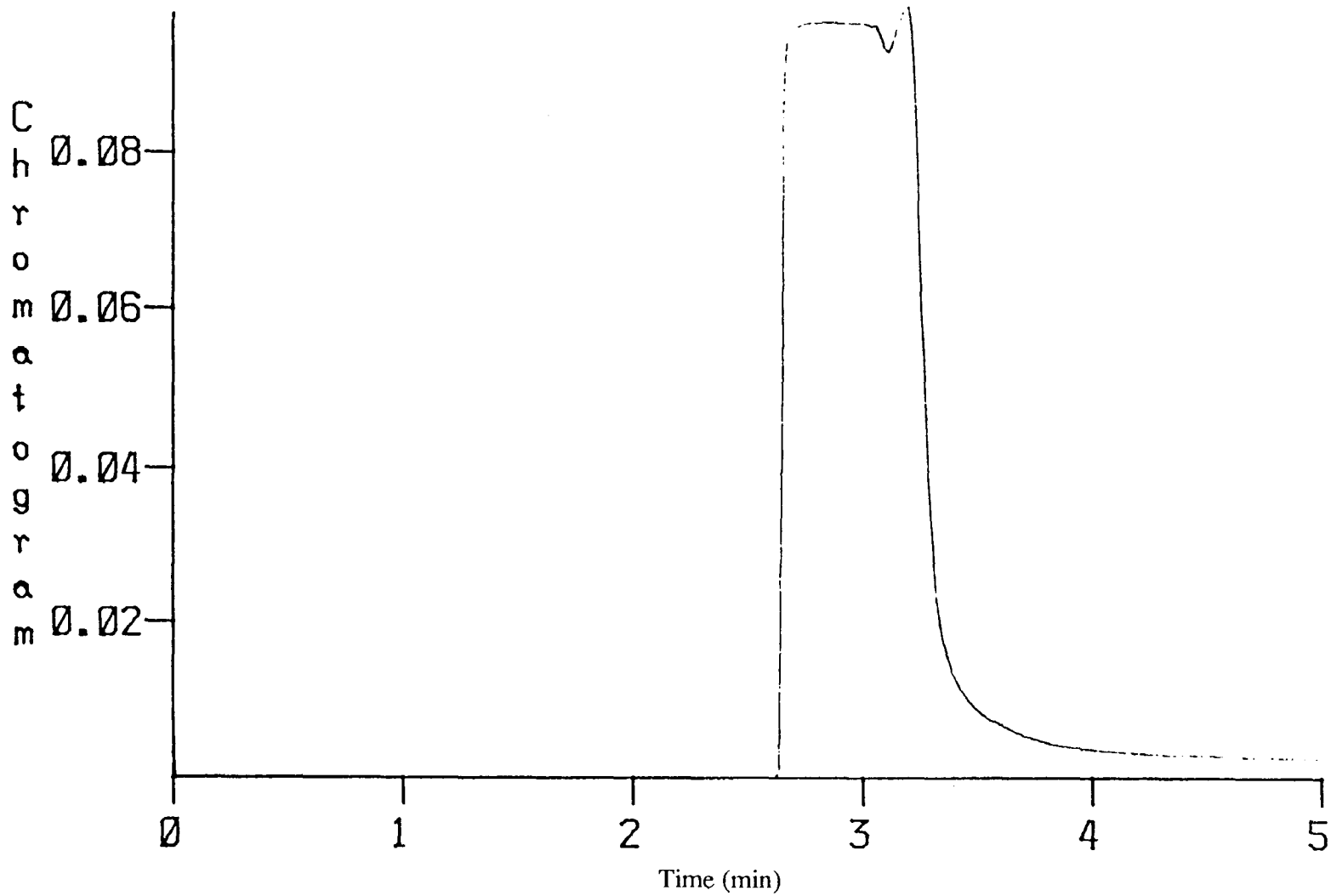

Figure 4.4 Chromatogram of NO_2 determination

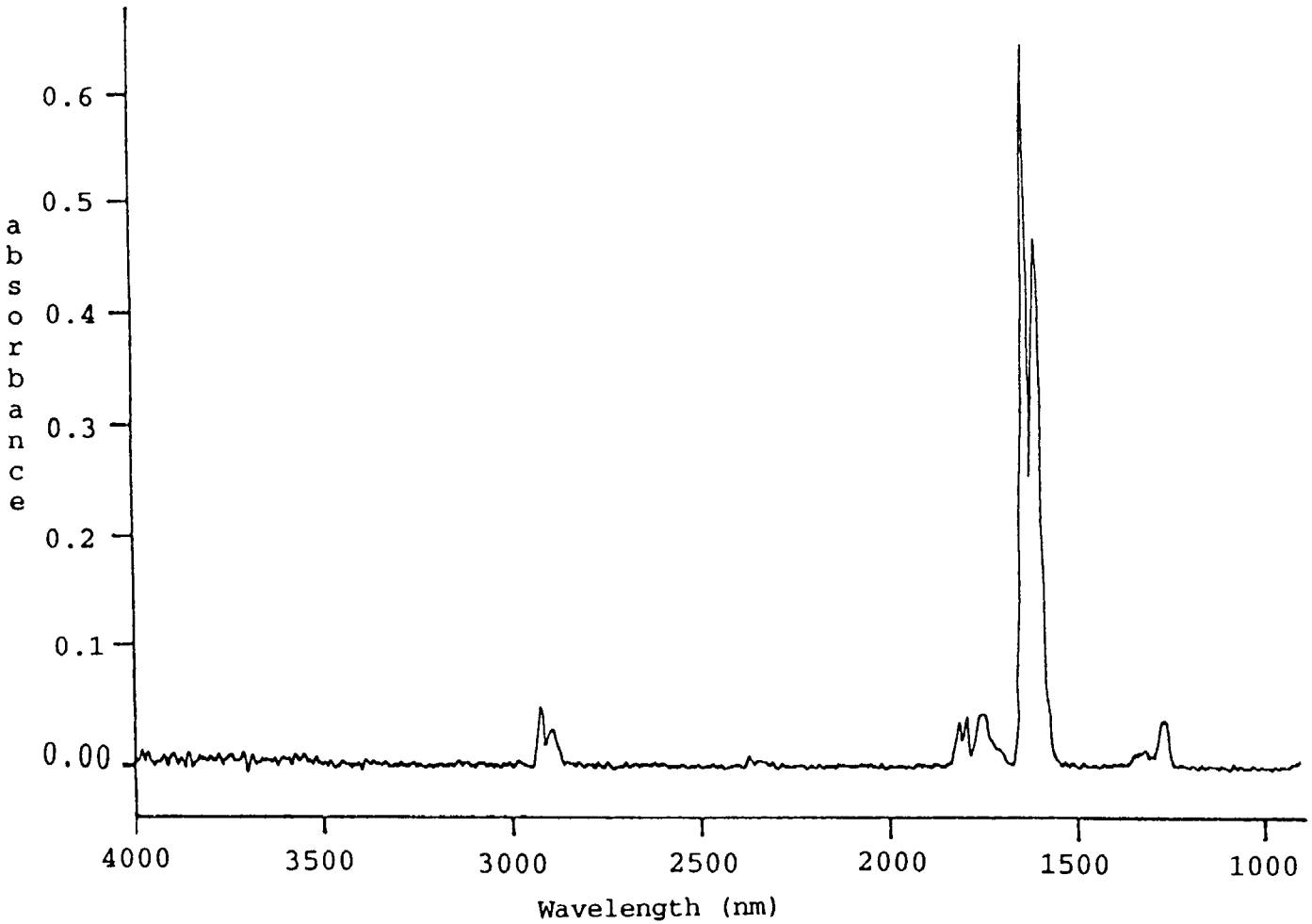

Figure 4.5 IR spectrum of 0.5 % of NO_2 in N_2

Two moles of NO_2 are equivalent to 1 mole of CaO. It was found experimentally that about 56 mg CaO is deposited on one gram of quartz wool. If we suppose that CaO is deposited on quartz wool uniformly, One can estimate that for the quartz used in this research, with the average fiber diameter is 9 ± 2 um that a uniform CaO layer would only be 0.199 ± 0.099 um. Thus, this system only involves the surface reaction and no bulk transport into CaO layers.

4.2.2.2 Effect of H_2O on Measurement of NO_2

It is very important to remove H_2O vapor in the operating mode 1 (Figure 3.2) before conversion of $Ca(NO_3)_2$ to CaO. If H_2O is left in the operating mode 1 (Figure 3.2), its IR absorbance will be added to the NO_2 concentration. Therefore, in the experiment, O_2 was allowed to pass through operating mode 1 (figure 3.2) to remove H_2O before the thermal conversion of $Ca(NO_3)_2$ to CaO. If the reactor temperature was kept at about 150 ^oC at the same time, H_2O IR absorbance still appeared in the IR spectrum during the NO_2 determination. The reason is that H_2O on the surface of quartz wool bonds to the quartz. Quartz wool is dehydrated over 300 ^oC. Therefore, at the same time that O_2 passes through operating mode 1 (Figure 3.2), the reactor temperature is kept at about 400 ^oC to make sure that quartz wool is dehydrated completely before the conversion of $Ca(NO_3)_2$ to CaO.

4.3 Results of FT-IR/GC Collection

This section presents the results using the GC data collection software as HCl reacts with CaO.

4.3.1 HCl Spectral Change

Figure 4.6 shows the overall IR spectrum of 4.9 % HCl in N_2. Only two bands, Vp(2) at 2842 cm^{-1} and Vp(3) at 2821 cm^{-1} were chosen for data acquisition.

At a given temperature, the intensities of the bands, Vp(2) at 2842 cm^{-1} and Vp(3) at 2821 cm^{-1}, decrease with time, indicating HCl reaction with CaO. Figure 4.7 shows that a series of HCl spectra recorded during the progress of the reaction at 400 ^{o}C as a function of time. Similar spectral patterns are obtained for reactions at 148, 175, 203, 248, 275, 300, 330, 356, 400 ^{o}C.

4.3.2 H_2O Spectral Change

According to the chemical equation

$$CaO + 2\ HCl \text{ ----> } CaCl_2 + H_2O,$$

the amount of H_2O vapor should increase during the progress of reaction. Figure 4.8 shows how the intensities of a series of H_2O vapor bands in the region 1665 to 1555 cm^{-1} increase with time during the progress of the reaction at 400 ^{o}C. Similar results are also obtained for reactions at 148, 175, 203, 248, 275, 300, 330, 356, 400 ^{o}C.

4.3.3 Dilution Effect

When the valves are switched from cycle 1 to cycle 2 (Figure 3.1), HCl gas is diluted. Therefore, the first drop in intensity at about 2 seconds is caused by dilution of HCl gas, not by the reaction. The dilution coefficient is 0.355.

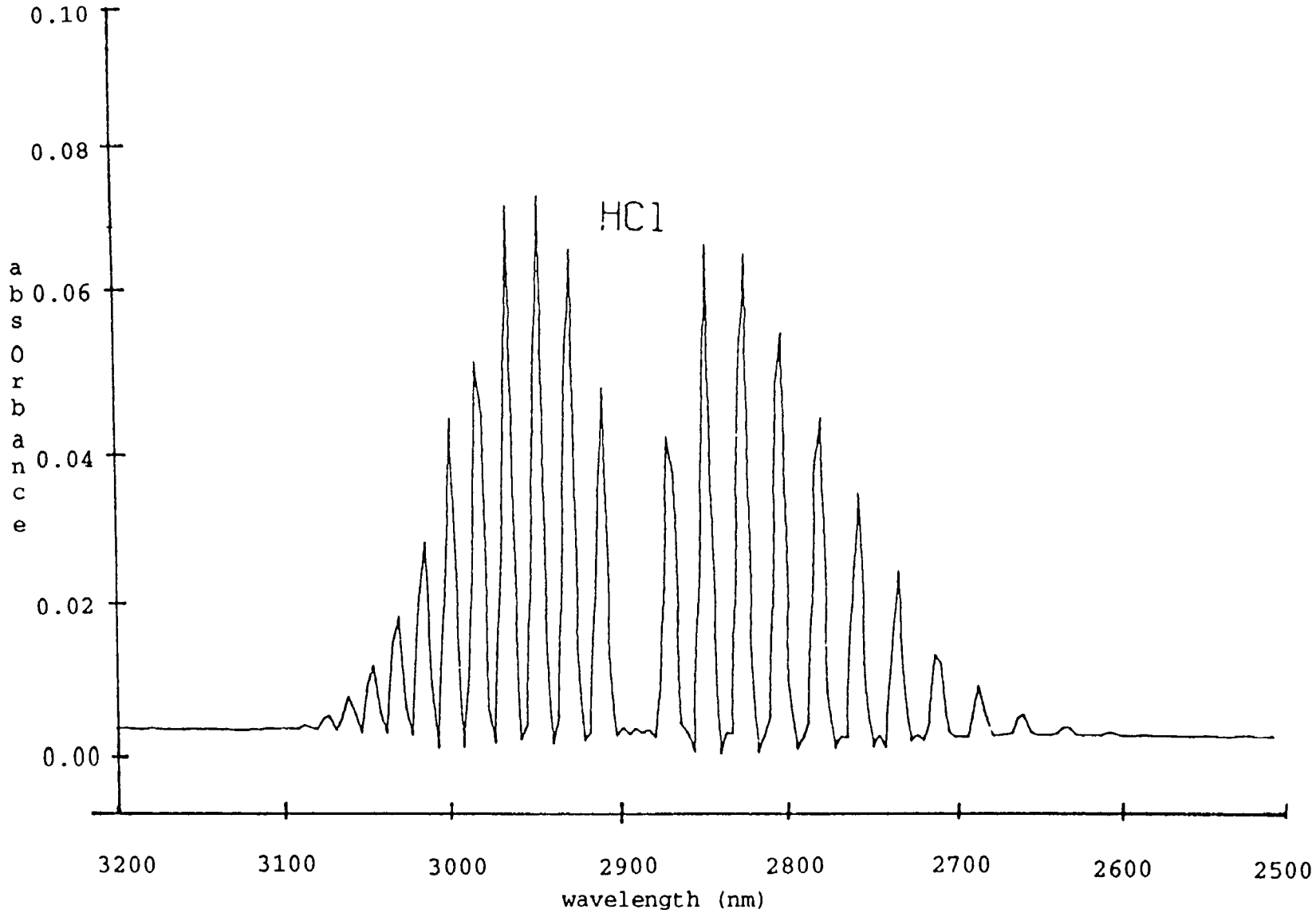

Figure 4.6 Overall IR spectrum of 4.9 % of HCl gas in N_2

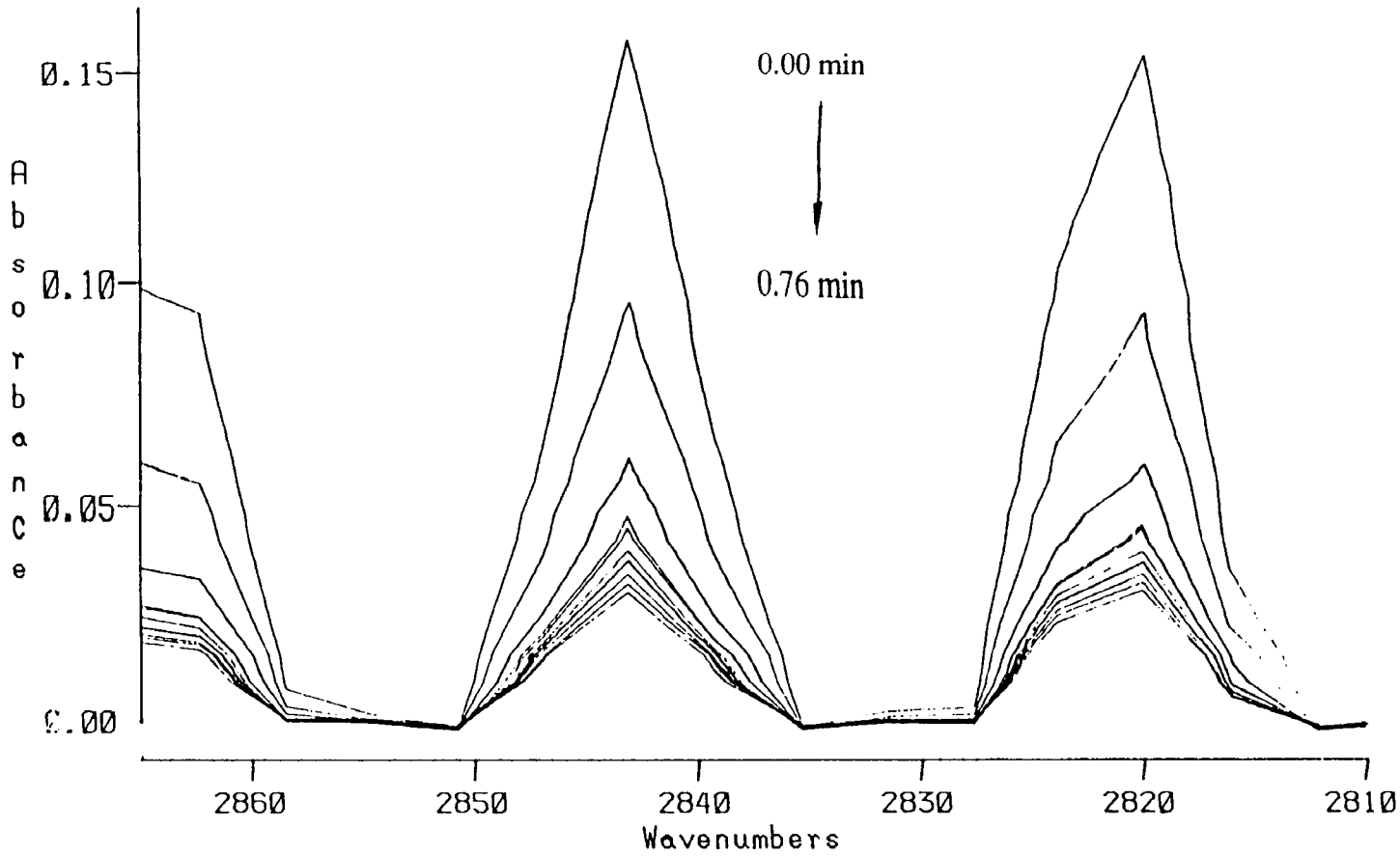

Figure 4.7 Time-dependent FT-IR spectra of the HCl gas bands (vp(2), vp(3) at 2842 cm^{-1} and 2821 cm^{-1} during HCl reaction with CaO deposited on quartz wool, at 400 ^{o}C

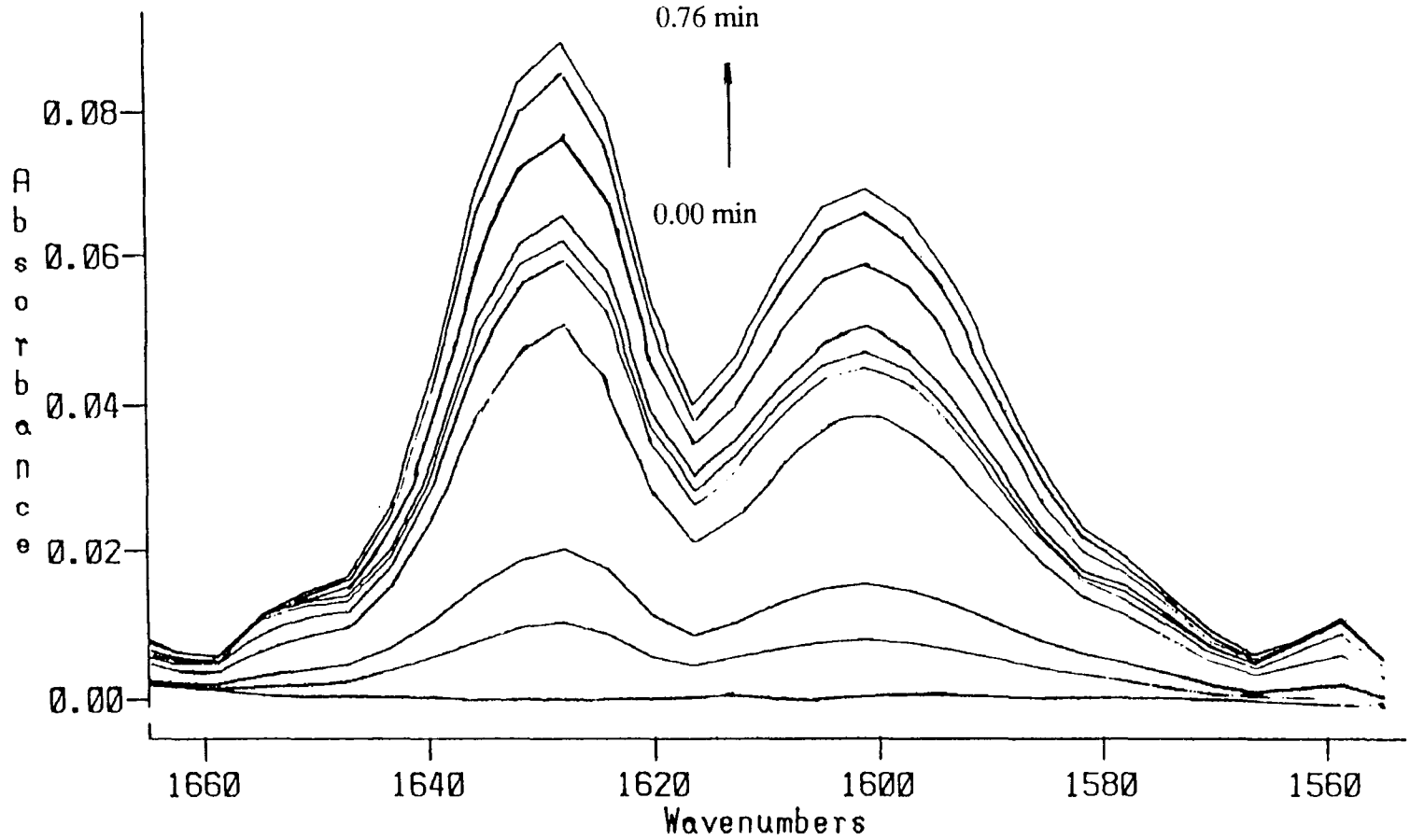

Figure 4.8 Time-dependent FT-IR spectra of H_2O vapor in the region from 1665 to 1555 cm^{-1} during reaction with CaO deposited on quartz wool, at 400 ^{0}C

4.4 Reaction of HCl with CaO

4.4.1 Mass Balance of HCl Gas

At the experimental condition used in this study, the reaction was carried out in cycle 2 (Figure 3.1), a batch operation, no HCl gas entered or left the reactor during the progress of the reaction. If m is the mass of HCl gas corresponding to zero concentration and Δx is the conversion in the system in time Δt, the accumulation of HCl in the system in time Δt is $-m\Delta x$. then, HCl mass balance may be written as

$$-rV\Delta T = -m\Delta x \tag{4-1}$$

where, V is volume of batch reactor system, and r reaction rate. The property of the HCl gas will vary with time, so that the mass balance becomes a differential equation. If we divide by Δt and take the limit as $\Delta t \rightarrow 0$, Eq.(4-1) become

$$dx/dt = rV/m \tag{4-2}$$

Because the experiment was carried under isothermal condition, reaction rate, r, is dependent only of composition (or conversion, for a single reactant), so that a solution of conversion with respect to time is obtainable from the mass balance alone. We can show the result by solving Eq.(4-2) for dt and integrating

$$t = -m\int_{x_1}^{x_2} \frac{dx}{rv} = -\frac{m}{m_t}\int_0^x \rho\frac{dx}{r} \tag{4-3}$$

where x_1 is the initial conversion, which equal zero, x_2 the conversion at any time t, m_t is total mass left at any time, and p density of HCl gas.

The volume change of solids caused by the formation of $CaCl_2$ is negligible relative to the volume of the reaction system, cycle 2 (Figure 3.1). The volume of HCl gas is consistent and conversion can be expressed as

$$x = \frac{C_0 - C}{C_0} \tag{4-4}$$

where C_0 is the initial concentration and equal to m/V. Equation (4-3) then becomes

$$t = -C_0 \int_0^x \frac{dx}{r} \tag{4-5}$$

Since r is a function of concentration or conversion of HCl. Therefore, x also can be expressed as a function of time

$$x = f(t) \tag{4-6}$$

4.4.2 Calculation of Conversion

Since the intensity of an IR absorbance band is proportional to the concentration of the component causing that band, the expression is written

$$A = aC \tag{4-7}$$

where A is absorbance of HCl, C concentration of the compound of interest, and a, the ratio constant, equal to multiplication of intensity of absorbance by path length,. Substituting Eq.(4-7) into Eq.(4-4), intensity of HCl absorbance can be converted to fractional conversion

$$x = \frac{A_0 - A_t}{A_0} \qquad (4\text{-}8)$$

where, A_0 is the initial intensity of HCl gas absorbance at 0 seconds, A_t the intensity of HCl gas absorbance at any time t. A_0 is determined by the calibration method described in section 4.3.4. Figure 4.9a and figure 4.9b is a plot of HCl conversion, x, with reaction time, t, and shows a parabolic increase of x with t at all temperatures from 148 to 400 ^{o}C. As the reaction temperature increases, the conversion also increases.

4.5 Studies of the Reaction Kinetics

The rest of this chapter is devoted to interpreting the chemical kinetics.

4.5.1 Reaction Order

The reaction under study could be represented by the general stoichiometric equation:

$$a\,A\,(g) + b\,B\,(s) \longrightarrow c\,C\,(g) + d\,D\,(s) \qquad (4\text{-}9)$$

In particular, the reaction under study is

$$2HCl + CaO \longrightarrow H_2O + CaCl_2 \qquad (4\text{-}10)$$

The stoichiometry of reaction was verified by X-ray diffraction analysis and from the maximum weight gain corresponding to full conversion of CaO to $CaCl_2$ [8].

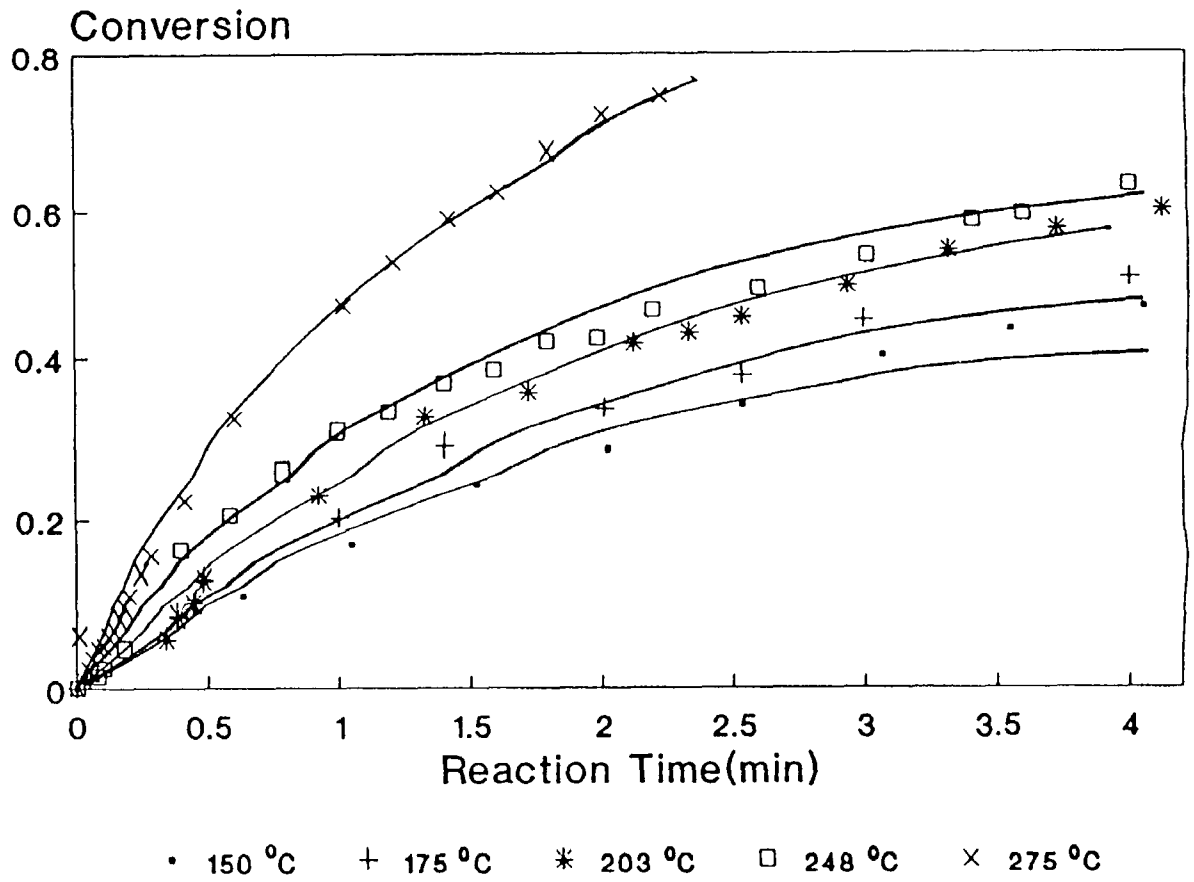

Figure 4.9a Temperature dependence on the reactivity of CaO towards HCl at temperatures of 150 to 275 ^{o}C

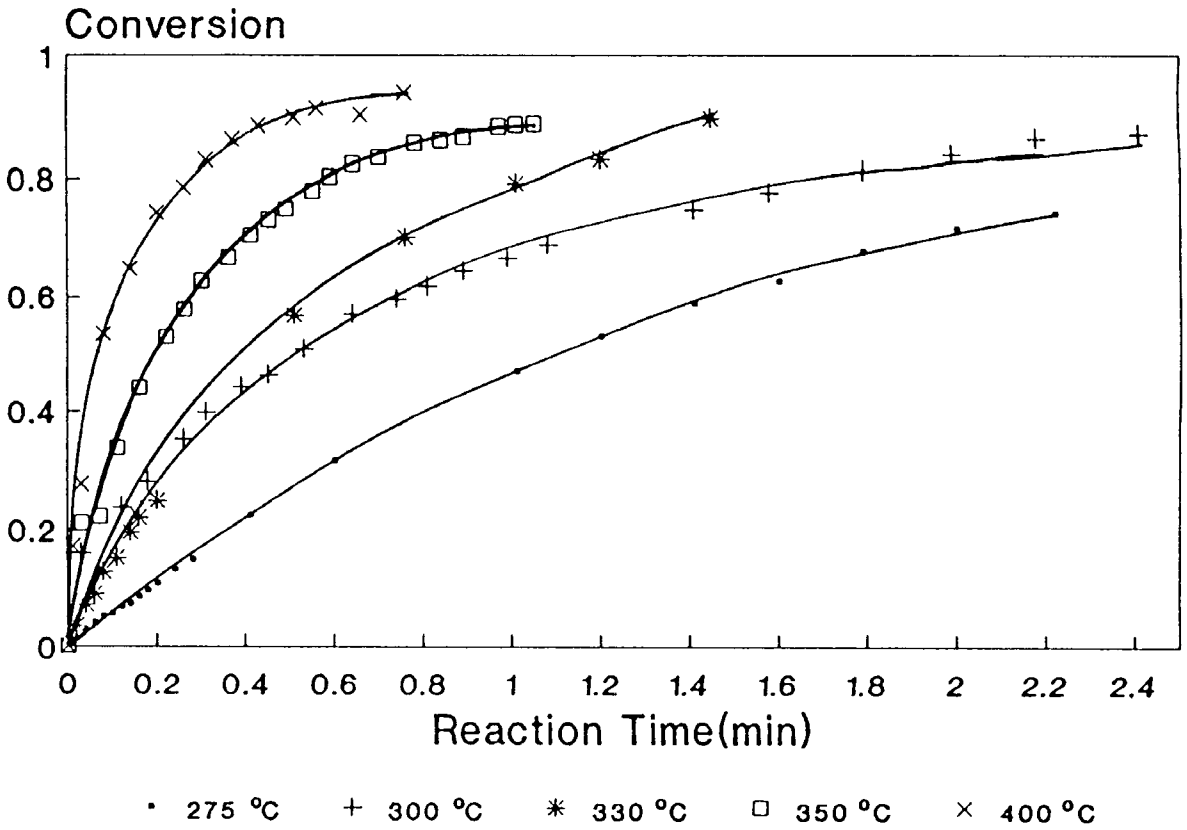

Figure 4.9b Temperature dependence on the reactivity of CaO towards HCl at temperatures of 275 to 400 ^{O}C

The order of a reaction has to be determined experimentally because it only coincides with the molecularity for elementary processes that actually occur as described by the stoichiometric equation. Only for elementary reactions is the order a small whole number. When the stoichiometric equation is an "overall" equation for a process consisting of several kinetic steps, the order cannot be predicted on the basis of stoichiometry only. The order may be a fraction or even a negative number.

The most common experimental procedure for establishing rate equations is to measure the composition of the reaction mixture at various stages during the progress of reaction. In a batch system, this means analysis at various times after the reaction begins. Then, the data are compared with various types of rate equations to find the one giving the best agreement.

The comparison can be made in two ways:

1. The integration method, comparison of predicted and observed compositions. For this approach it is necessary to integrate the rate expression to give concentration as a function of time.
2. The differential method, comparison of predicted and observed rates. The latter are obtained by differentiating the experimental data.

According to the properties of the reaction system we used, the volume reaction model was used to analyze reaction kinetics of HCl with CaO. The shrinking core model was used to investigate reaction equation by B.K. Gullett et al.[7] and grain model by M. Daoudi et al.[5, 8]. Their results show that the reaction is first order with respect to the

concentration of HCl gas even if under the condition that the reaction is not controlled by only chemical resistance. However, in our research, CaO deposited on quartz wool in a very thin film, only about 0.199 um if we supposed that CaO was deposited on quartz wool uniformly, was visualized as consisting of a number of very small, very porous particles as a "volume reaction model" or "dispersed-solid model". The gas reactant can penetrate into the solid and the reaction may be assumed to take place all over the volume of the particles rather than at a sharp interface. This is equivalent to having a monolayer of CaO. At relative low temperatures, intrinsic rate resistance would be significant and mass transfer and pore diffusion resistance would be negligible. Moreover, the high speed pump employed in this study also largely minimized the effect of mass transfer and pore diffusion.

Under the above assumption and taking account of reaction order with respect to the gas phase, the intrinsic reaction expression can be written as follows

$$\overline{R}_A = -k_V C_B^M C_A^N \qquad (4\text{-}11)$$

where, k_V is the reaction rate per unit volume of sorbent, M reaction order of component B and N reaction order of component A. For the reaction studies here, assume M, N are one.

For the reaction of Ca-based sorbent with HCl, first-order reaction with respect to HCl concentration has been reported by three literature references, using three different methods. In the case of first order reaction with respect to gas reactant, there is no need to consider the presence of a completely reacted product layer because the concentration

of solid reactants can approach zero only as time approaches infinity. Moreover, the concentration of CaO is much larger than that of HCl gas. Therefore, assuming

$$k_V C_B^M = k' \tag{4-12}$$

Substituting eq.(4-12) into eq.(4-11), the reaction rate can be expressed as

$$\overline{R}_A = -k' C_A \quad \text{or} \quad \frac{dC_A}{dt} = -k' C_A \tag{4-13}$$

where, k' is the pseudo first order rate constant, C_A represents concentration of HCl gas. Then, according to Eq.(4-8), the integrated result is

$$\ln \frac{C_A}{C_0} = -k' t \tag{4-14}$$

substituting Eq.(4-8) into Eq.(4-13) yields

$$\ln(1-x) = -k't \tag{4-15}$$

Figure 4.10a and figure 4.10b shows that the experimental results is quite consistent with first order reaction with respect to HCl concentration at the temperature from 148 ^{o}C to 400 ^{o}C.

4.5.2 Effect of Temperature on Rate Constant

The rate constants determined from slope of lines in Figure 4.10a, b were found to match the Arrhenius expression. A plot of the results obtained is shown on Figure 4.11. the activation energy computed from the slope of the best fit line was found to be 7490 cal/mol with a corresponding frequency factor of 0.241/min·mg leading therefore to the following relation expressing the effect of temperature on the rate constant as

$$k_v = 0.241\exp(-7490/RT) \qquad (5\text{-}15)$$

where T is the absolute temperature and R the universal gas constant (R = 1.987 cal/mol.K).

The activation energy reported here is larger than the activation energy reported by other authors for reaction of Ca-based sorbents with CaO. Among these authors, Daoudi et al. [8] calculated an activation energy of 5300 cal/mol for the system $CaCO_3$/HCl under the chemical control and mass transfer control. Weinell et al. [6] reported an activation energy of the range from 2390 to 3585 cal/mol under the control of pore diffusion and mass transfer. G.K Gullett et al. [7] investigated the reaction of CaO with HCl at the temperature from 148 ^{o}C to 350 ^{o}C under the condition that minimized bulk mass transfer and pore diffusion limitation. The activation energy they reported is 6692 cal/mol. Our result of activation energy is 7490 cal/mol, which is higher than those of B.K Gullett et al.[7], but is probably more representative of a true surface reaction.

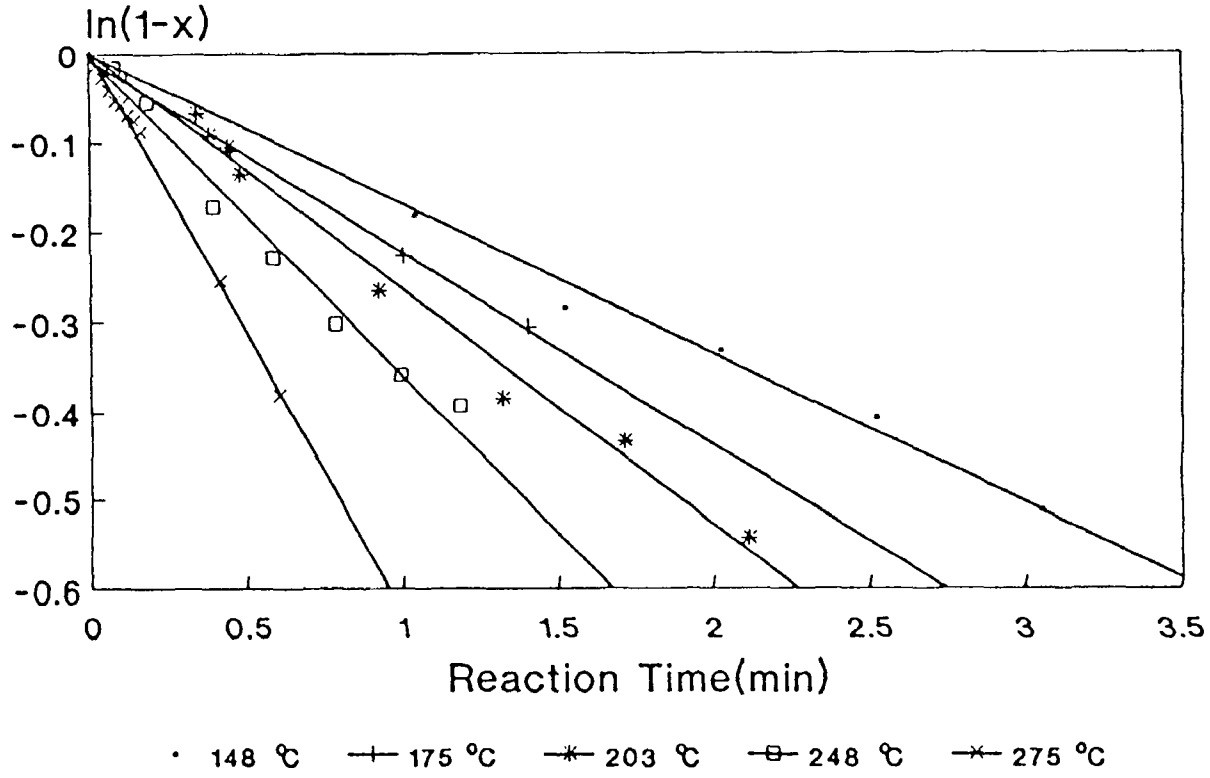

Figure 4.10a Plot of ln(1-x) with time from the temperature 148 to 275 ^{o}C

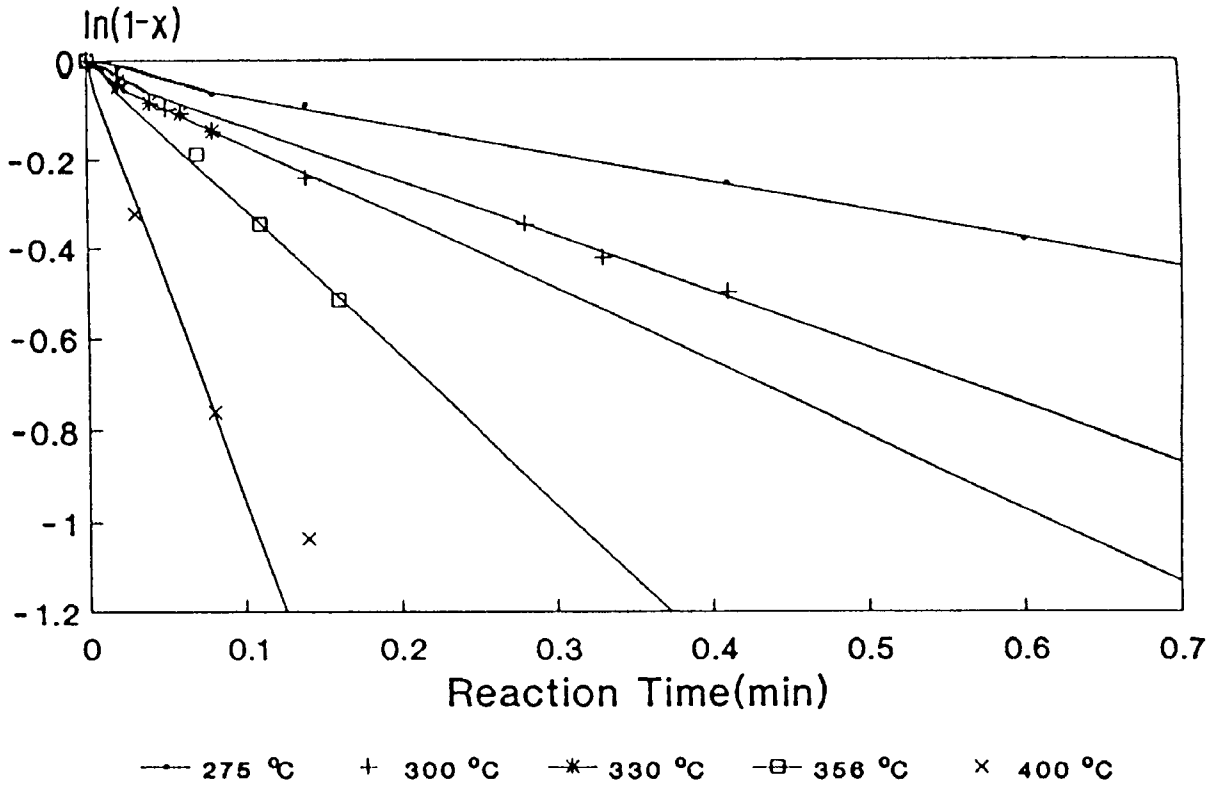

Figure 4.10b Plot of ln(1-x) with time from the temperature 275 to 400 ^{o}C

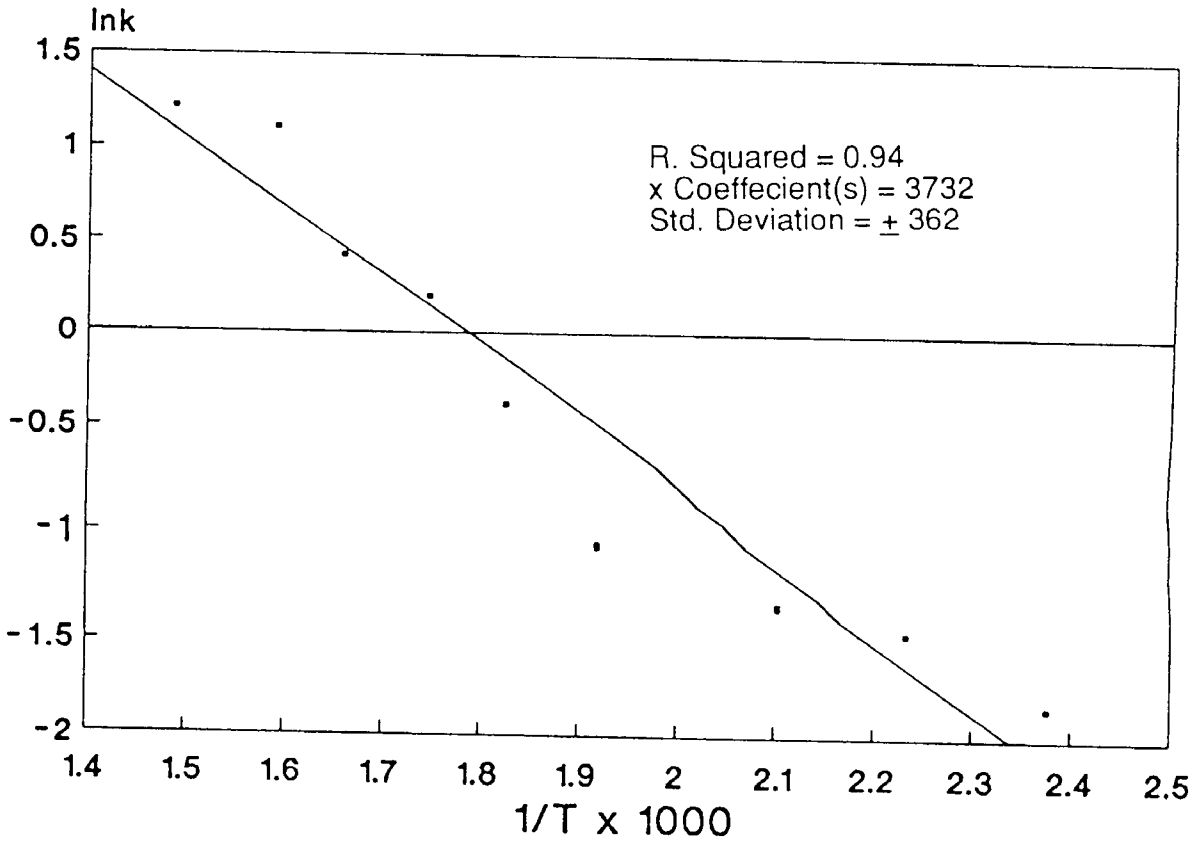

Figure 4.11 Arrhenius plots for the reaction of HCl with CaO

4.5.3 Effect of Mass transfer and Pore Diffusion

B.K Gullett et al [7] show that the kinetics of the reaction between CaO particles and a mix of HCl in nitrogen led to an apparant activation energy of 6692 cal/mol when potential bulk mass transfer and pore diffusion limitation were minimized. They used reactive gas flow condition sample sizes, and HCl concentration minimized external film diffusion resistant on kinetics. The criteria used Ranz and Marshall [13] requiring the Sherwood number to remain about 2 and Levenspiel 's [14] criteria for eliminating pore diffusion control.

Weinell et al., [6] also estimated external diffusion and showed that they are much faster than the kinetics of the HCl-CaO reaction and therefore do not affect the measurement.

Since our results agreed with Gullett 's et al. [7] et al. [6] 's data in basis of being first order with respect to HCl concentration and we obtained a slightly higher activation energy of 7490 cal/mol, we assumed that bulk mass transfer and pore diffusion were not affecting our results.

CHAPTER FIVE

CONCLUSIONS

The reaction kinetics of CaO with HCl from 148 to 400 ^{o}C were studied under conditions minimizing mass transfer and pore diffusion limitations with the use of FT-IR spectroscopy. The reaction was carried out in a closed system. The initial concentration of HCl was about 1.74 % and that of CaO about 28 mg. The CaO was dispersed over 0.5 gram of quartz wool, corresponding to a calculated thickness of about 15 um. The conclusion from this research are

1 From the real-time data, it is verified that HCl reaction with CaO is a first-order reaction with respect to HCl concentration.

2 In the temperature from 148 to 400 ^{o}C, the chemical reaction rate constant obeys the Arrhenius expression with an activation energy of 7490 kJ/mol.

3 This research demonstrates how FT-IR with GC-32 software can be efficiently applied to real-time monitoring of gas-solid reactions

4 Real-time data allow the determination of kinetics with good precision and reproducibility

CHAPTER SIX

RECOMMENDATION

The results presented in this thesis indicate that the reaction system designed and set up for investigating of kinetics of HCl with CaO worked very well. At the conditions used in this research, we found that we could minimized mass transfer and pore diffusion. This system can be used for other gas/solid reactions. However, further research still needs to be conducted in the following areas:

1. Utilization of CaO dispersed on quartz wool
2. Effect of recirculating rate on minimizing the effects of mass transfer and pore diffusion at different reaction temperatures.
3. Investigation of the kinetics of HCl with CaO at temperature over 400 ^{o}C.
4. Observing the change of solid phase weight with time by TGA during the progress of the reaction and comparing the kinetic results with these using FT-IR.
5. Scaling up to continuous flow reactor and seeing the effect of residence time on conversion and whether the kinetics from continuous flow reactor fit the model from the batch system.
6. The possibility of high temperature removal of HCl with MgO and regeneration of $MgCl_2$ with water to concentrated HCl and MgO.

APPENDIX 1

Table 1 Data for time-conversion and reaction order

at 148 ^{o}C

Time (min)	Absorbance	Conversion	ln(1-x)
0.57	0.0463	0.094	-0.099
0.98	0.0433	0.145	-0.157
1.46	0.0391	0.217	-0.245
1.96	0.0373	0.248	-0.284
2.46	0.0345	0.294	-0.348
2.99	0.0311	0.352	-0.434
3.47	0.0293	0.383	-0.482
3.97	0.0276	0.410	-0.528
4.45	0.0254	0.448	-0.594
4.97	0.0245	0.464	-0.624
5.47	0.0213	0.518	-0.729
5.95	0.0209	0.524	-0.743

at 175 ^{o}C

Time (min)	Absorbance	% Conversion	ln(1-x)
0.05	0.0565	0.012	-0.012
0.45	0.0513	0.104	-0.11
1.0	0.0457	0.201	-0.225
1.4	0.0408	0.286	-0.305
2	0.0383	0.33	
2.52	0.0358	0.375	
2.98	0.0315	0.45	
3.98	0.0281	0.508	

at 203 ^{o}C

Time (min)	Absorbance	% Conversion	ln(1-x)
0	0.0592	0	0
0.34	0.0554	0.0651	-0.0673
0.38	0.0541	0.0869	-0.0909
0.44	0.0533	0.0997	-0.105
0.48	0.0517	0.126	-0.135

Table 1 (cont.)

0.92	0.0455	0.232	-0.265
1.32	0.0403	0.319	-0.384
1.71	0.0384	0.352	-0.434
2.11	0.0344	0.418	-0.542
2.32	0.0336	0.433	
2.52	0.0323	0.455	
2.92	0.0298	0.497	
3.30	0.0270	0.545	
3.71	0.0252	0.575	
4.11	0.0236	0.601	

at 248 ^{o}C

Time	Absorbance	% Conversion	ln(1-x)
0	0.150	0.00	0
0.08	0.0532	0.0158	-0.0159
0.10	0.0526	0.0257	-0.0261
0.18	0.0511	0.0533	-0.0548
0.39	0.0455	0.158	-0.172
0.58	0.0430	0.205	-0.229
0.78	0.0399	0.261	-0.302
0.99	0.0378	0.301	-0.358
1.18	0.0365	0.325	-0.393
1.39	0.0344	0.364	
1.58	0.0334	0.382	
1.78	0.0313	0.421	
1.97	0.0311	0.425	
2.16	0.0290	0.463	
2.56	0.0274	0.493	
2.99	0.0250	0.538	
3.39	0.0224	0.586	
3.58	0.0219	0.595	
3.98	0.0197	0.635	
4.39	0.0187	0.654	
4.75	0.0178	0.670	

at 275 ^{o}C

Time (min)	Absorbance	% conversion	ln(1-x)
0	0.0532	0	0
0.04	0.0518	0.027	-0.028
0.06	0.0510	0.041	-0.042
0.08	0.0504	0.052	-0.054
0.1	0.502	0.056	-0.058

Table 1 (cont.)

0.12	0.0496	0.067	-0.069
0.14	0.0493	0.073	-0.076
0.16	0.0487	0.085	-0.089
0.41	0.0412.	0.225	-0.255
0.6	0.0363	0.317	-0.381
1.01	0.0282	0.470	
1.2	0.0250	0.530	
1.41	0.0219	0.589	
1.6	0.0199	0.626	
1.79	0.0172	0.676	
2	0.0151	0.716	
2.22	0.0138	0.741	

at 300 ^{o}C

Time (min)	Absorbance	% Conversion	ln(1-x)
0	0.0568	0	0
0.05	0.0521	0.083	-0.087
0.14	0.0446	0.215	-0.242
0.28	0.0402	0.293	-0.347
0.33	0.0373	0.344	-0.421
0.41	0.0345	0.392	-0.497
0.45	0.0305	0.463	
0.53	0.0280	0.508	
0.64	0.0244	0.57	
0.74	0.0230	0.595	
0.81	0.0218	0.617	
0.89	0.0202	0.644	
0.99	0.0190	0.666	
1.08	0.0177	0.688	
1.41	0.0143	0.748	
1.58	0.0127	0.776	
1.79	0.0107	0.812	
1.99	0.0092	0.838	
2.18	0.0077	0.864	
2.41	0.0074	0.87	

at 330 ^{o}C

Time (min)	Absorbance	% Conversion	ln(1-x)
0	0.0554	0	0
0.02	0.0534	0.036	-0.037
0.04	0.0515	0.071	-0.073

Table 1 (cont.)

0.06	0.0504	0.091	-0.095
0.08	0.0483	0.128	-0.137
0.2	0.0416	0.249	
0.51	0.0240	0.567	
0.76	0.0166	0.701	
1.01	0.0116	0.791	
1.2	0.0095	0.829	
1.45	0.0058	0.895	

at 356 ^{o}C

Time (min)	Absorbance	% Conversion	ln(1-x)
0	0.0554	0	0
0.03	0.0437	0.211	-0.237
0.07	0.0431	0.222	-0.251
0.11	0.0367	0.337	-0.411
0.16	0.0310	0.440	-0.579
0.22	0.0262	0.528	-0.750
0.26	0.0235	0.576	-0.858
0.3	0.0208	0.625	
0.36	0.0185	0.665	
0.41	0.0164	0.703	
0.45	0.0150	0.728	
0.49	0.0140	0.742	
0.55	0.0123	0.777	
0.59	0.011	0.801	
0.64	0.0099	0.821	
0.7	0.009	0.820	
0.78	0.00798	0.856	
0.89	0.0075	0.865	
0.97	0.0065	0.882	
1.01	0.0063	0.885	

at 400 ^{o}C

Time (min)	Absorbance	% Conversion	ln(1-x)
0	0.0534	0	0
0.03	0.0386	0.277	-0.325
0.08	0.0249	0.534	-0.763
0.14	0.0189	0.646	-1.039
0.2	0.0138	0.742	
0.26	0.0115	0.785	
0.31	0.0092	0.828	

Table 1 (cont.)

0.37	0.0074	0.861
0.43	0.0063	0.883
0.51	0.0055	0.897
0.56	0.0047	0.911
0.66	0.0043	0.920
0.76	0.0033	0.938

Note:
1. Initial absorbance at t = 0 is equal to initial absorbance readings multiplying dilute coefficient 0.355.
2. data obtained at 400 ^{o}C is that the experiment was carried out on 112 mg of CaO on 1 gram quartz wool.

Table 2 Data for the Ahrrenius plot

Temperature ^{o}C	K	1/T	k'	lnk'
400	673	0.001485	4.16 $\pm$ 0.05	1.209
356	629	0.001589	3.12 $\pm$ 0.20	1.102
330	603	0.001658	1.66 $\pm$ 0.08	0.418
300	573	0.001745	1.17 $\pm$ 0.08	0.196
275	548	0.001824	0.632 $\pm$ 0.012	-0.380
248	521	0.001919	0.357 $\pm$ 0.018	-1.033
203	476	0.002100	0.273 $\pm$ 0.013	-1.328
175	448	0.002232	0.216 $\pm$ 0.006	-1.448
148	421	0.002375	0.131 $\pm$ 0.009	-1.835

Appendix 2

GC-32 Software

This section will give the introduction about GC-32 software following the GC-32 Operation 's Manual (BIO-RAD).

1. Kinetic Studies using GC-32 Software

The GC-32 software is designed for kinetic studies. Kinetic studies measure spectroscopic changes as a function of time, and involve collecting a series of spectra through an entire experiment at a rate that resolves the changes of interest. The species whose spectra can be obtained in this way could be reaction intermediates or elution fractions. Several kinetic experiments are listed below.

kinetic experiments classified by required time resolution:

	Time Resolution	Applications
I.	Greater than 30 seconds	Sample cure & thermal degradation
II.	6-30 seconds	Evolved gas analysis & LC/IR
III.	1-6 seconds	Packed & capillary GC/IR
IV.	0.16-1 seconds	Sample deformation (e.g. polymer stretching)
V.	Less than 0.1 second	Gas phase reactions (e.g. flashlamp or laser photolysis)

Time resolution is determined by the frequency of data collection. Using an MCT detector, scanning at 20 KHz and a spectral resolution of 8 cm^{-1}, collection of four scans requires about 1 second. These 4 scans, when coadded, form a single scan-set. If 2 seconds time resolution (i.e.

one spectrum every 2 seconds) is desired, then 8 scans would be coadded per scan set. While the kinetics experiment is in progress, the specified number of scans are coadded to produce a scan-set, and this scan-set is then saved on the Winchester disk.

2. GC-IR Data Collection

In the data collection step we obtain a complete IR spectroscopic record of the GC run. GC/IR data collection must keep pace with the GC resolution, and most GC peaks separated by a capillary column have half-widths between 1 to 5 seconds. Several scans should be collected per peak, and therefore IR spectra (scan-sets) are collected at about one per second.

When the GC/IR run is in progress, the spectrometer coadds the specified number of interferograms into a scan-set. Without an array processor, the interferogram is transformed and low resolution (32 cm^{-1}) absorbance spectra computed while the collection proceeds. Only the interferogram data is saved. A separate compute step is used after data collection to calculate 8 cm^{-1} absorbance spectra. In the case of an array processor collect, the interferogram is transformed and 8 cm^{-1} absorbance spectra computed while collection proceeds. Only the absorbance spectra are saved and not the interferograms. This compresses the stored data and eliminates a separate, post-collect, compute step.

Historically, GC/FT-IR data was collected in two ways. One method was to continuously collect IR data for the entire GC run, and the other employed "thresholding." Thresholding attempted to save only the data where there was significant attenuation of the IR beam. The

thresholding method was developed to accommodate the limited data storage capacities of early mini-computer disks and floppy-based microprocessor systems. Thresholding had the major disadvantage of omitting useful data; such as not always collecting IR data from small peaks in the chromatogram. However, data storage capacities have advanced, allowing the storage of the entire GC run. For this reason, GC/32 software does not employ thresholding. All scan-sets are collected and stored for processing, eliminating the possibility of missing important data.

3. Reconstructed Chromatograms

IR reconstructed chromatograms greatly facilitate the data reduction procedure of producing GC-IR spectra. IR reconstructed chromatograms are created from both spectra (functional group chromatograms, FGC) and from interferograms (Gram-Schmidt chromatograms, GSC). A FGC is a plot of absorbance at a certain frequency versus time after sample injection. During data collection, a set of FGCs are created by Fourier transforming points from each collected scan-set and using the 32 cm^{-1} spectra obtained. In system using an array processor, the actual 8 cm^{-1} spectra are used to create the real-time FGCs.

The FGCs are useful for identifying GC fractions belonging to a particular chemical class (esters, alcohols, etc.) in a complex mixture. GC-32 allows a maximum of five FGC regions to be specified. The system is shipped with a default set of FGC regions, but another set may be used. Specific knowledge of the composition of your sample aids in determining the FGC regions to be defined.

The GSC is created directly from the interferogram using the Gram-Schmidt orthogonalization process. The G-S orthogonalization process produces an orthogonal set of basis vectors from a linear indendent set of vectors. The linear independent set of vects is a reference subspace created by collecting a number of interferograms with only the carrier gas flowing through the light pipe. When a GC fraction passes through the light pipe, a sample vector is created from the sample interferogram. The Euclidean distance of the sample vector from the reference subspace depends upon absorbances in the light pipe. Applying Beer 's law, the absorption of light is an exponential function of the concentration of the absorbing substance present. Under favorable conditions, the GSC can be used for semi-quantitative determinations.

The GSC greatly facilitates the data reduction procedure. Components separated by the GC appear in the GSC and indicate which scan-set will produce useful IR spectra. The GSC complements the traditional GC detector because most peaks that occur in the GSC appear in the flame ionization detector (FID) chromatogram. However, for the majority of compounds the FID is much more sensitive than the GSC, so that not every peak in the FID will produce a significant IR spectrum. We want to find scan-sets with significant IR absorbances. Therefore, we want to examine an IR-based chromatogram: the GSC. Furthermore, a time delay exists between when the FID produces an ion current and when the compound passes through the light pipe. The difference would make peak editing based on FID chromatograms more difficult.

The FGCs further enhance the process of defining chromatogram peaks. A compound separated with the gas chromatograph may appear to be a single peak from the GSC, but when analyzed at a more specific spectral range is shown to be more than one peak. The FGCs can also reveal a shoulder in a peak that appears merged in the GSC.

4. An Overview of A GC/IR Run

A GC/IR experiment follows a basic sequence. In this section, Two efficient and productive experimental processes, non-array processor and array processor will be discussed in this section.

4.1. Non-array processor GC/IR outline

setting up the run

Start the GC experiment by examining and updating parameter values. The GC-32 package provides an initial parameter set which simplifies the task. Setting up the run also includes checking the interferogram and running a 100 % line. Both of these measures check system stability.

GC Collect

The GC/IR run begins with data collection. In data collection we obtain a complete FT-IR record of the run. First, the background spectrum (the spectrum of the "empty" lightpipe) is collected and stored. Then, the sample is injected and data collection resumes. The spectrometer continuously scans, and data is collected. The individual scans are coadded to meet the specified time resolution. The 3200 data system calculates the low resolution (32 cm-**1**) absorbance spectrum and GSC

point for each scan-set and displays them both on the monitor. The absorbance spectrum is then used to produce the five FGCs, one of which is displayed on the monitor. Thus, the GSC, one low resolution FGC and the low resolution absorbance spectrum for each scan-set are continuously displayed and updated as the run proceeds. The interferograms, FGCs and the GSC are stored for later processing.

Peak find

After data collection, the peak find command processes the GSC or a FGC and locates peaks, i.e. scan-sets where there are significant IR absorbances. The peaks are indexed by retention times and are stored for processing. The list of peak retention times is called a peak table. From the GC-32 menu, the peak find commend is executed from the "peak edit parameter page".

Peak edit

The peak edit command allows interactive editing of the GC/IR data, and begins where the peak find command left off. The automatic peak finder can miss scan-sets with low IR absorbances and create peaks where the separation may not be complete.

Peak edit has three interactive display modes: chromatogram mode, peak table mode and absorbance mode. Each display mode contains a main window, a radar box, plus an auxiliary window above the main window. The contents of each display window varies between the three peak edit modes. The GSC and FGCs are displayed in the chromatogram mode. The absorbance spectrum mode displays the absorbance spectrum of individual peaks or scan-sets and the GSC or a

FGC. The peak table mode displays the peak table and the GSC or a FGC.

From the chromatogram mode display, the user defines new peaks and backgrounds, redefines peaks and deletes peaks. Plus, absorbance spectra are computed for the chromatogram peaks. The editing occurs directly from the chromatogram mode display field. The current peak is marked on the displayed chromatograms; plus the chromatograms can be simultaneously rolled and zoomed for a closer examination. Editing functions are performed using the displayed chromatograms and single-key commands. For example, the peaks and backgrounds are defined by moving the cursor through the chromatograms and then pressing an assigned function key. Peaks containing limited IR interest (e.g. the solvent front) are deleted from the peak table. Background regions are defined to compensate for poor spectrometer purge, column bleed, incomplete chromatographic separations, etc. Every peak is assigned a background spectrum which is divided into the sample (peak) spectrum when the peak is computed to produce the absorbance spectrum. The peak table is automatically updated for each edit made to the chromatograms.

From the absorbance mode display, the absorbance spectrum of individual peaks or low resolution (32 cm-**1**) scan-sets are zoomed and rolled for a closer examination.

From the peak table mode, detailed peak information is given.

GC Compute

The GC computer command computes an absorbance spectrum for every peak in the peak table. (From the peak editor, individual

absorbance spectra can be computed for defined peaks.) The GC compute command takes the peak table as input, coadds the selected interferogram scan-sets, Fourier transforms the sample and background interferograms into single-beam spectra, divides the sample spectra by the appropriate background spectra and then computes the peak absorbance spectra.

Peak print

After editing the chromatograms and computing all the absorbance spectra, a hard-copy of the peak table should be made. The peak print command prints the peak table.

Save run

The save run command stores the spectral information created during the GC run under a selected name. It does not save the GC raw data. If the command is not run, all data is overwritten by the next GC run.

Spectral search

After the absorbance spectra have been computed and the GC run has been saved, the spectral search command identifies the peaks. It compares the absorbance spectra with a spectral library of known vapor phase compounds and finds the best matches. After completing the search, the best match spectra from the library are displayed alongside the unknown spectra. Also, the search package can produce single page plots showing both the unknown spectrum and best match spectra from the library.

Plotting Spectra and GSC

Plotting commands and quick plot formats for the GSC, absorbance spectra and search spectra are provided.

4.2 Array Processor GC/IR Outline

Setting up the run

Same as non-array processor.

GC collect

The GC/IR run begins with data collection. In data collection we obtain a complete FT-IR record of the run. First, the background spectrum (the spectrum of the "empty" lightpipe) is collected and stored. Then, the sample is injected and data collection resumes. The individual scans are coadded to meet the specified time resolution. The 3200 data system calculates the 8 cm-**1** absorbance spectrum and GSC point for each scan-set and displays them both on the monitor. The absorbance spectrum is then used to produce five FGCs, one of which is displayed on the monitor. Thus, the GSC, one FGC and the absorbance spectrum for each scan-set are continuously displayed and updated as the run proceeds. The absorbance spectra, five FGCs and the GSC are stored for later processing. The interferograms are not saved.

Peak find

Same as that of non-array processor.

Peak edit

The peak edit command allows interactive editing of the GC/IR data, and begins where the peak find command left off. The automatic peak finder can miss scan-sets with low IR absorbances and create peaks where the separation may not be complete.

Peak edit has three interactive display modes: chromatogram mode, peak table mode and absorbance mode. Each display mode contains a main window, a radar box, plus an auxiliary window above the main window. The contents of each display window varies between the three peak edit modes. The GSC and FGCs are displayed in the chromatogram mode. The absorbance spectrum mode displays the absorbance spectrum of individual peaks or scan-sets and the GSC or a FGC. The peak table mode displays the peak table and the GSC or a FGC.

From the chromatogram mode display, the user defines new peaks and backgrounds, redefines peaks, and deletes peaks. Plus, the absorbance scan-sets are coadded for the chromatogram peaks. The editing occurs directly from the chromatogram mode display field. The current peak is marked on the displayed chromatograms; plus the chromatograms can be simultaneously rolled and zoomed for closer examination. Editing functions are performed using the displayed chromatograms and single key commands. For example, the peaks and backgrounds are defined by moving the cursor through the chromatograms then pressing an assigned function key. Peaks containing limited IR interest (e.g. the solvent front) can be deleted from the peak table. Backgrounds regions are defined to compensate for poor spectrometer purge, column bleed, incomplete chromatographic

separations, etc. A background region is assigned to every peak. A background region, when GC data is collected with an array processor, is actually an absorbance spectrum. This absorbance spectrum is subtracted from an assigned peak to compensate for interferences. When a background region other than the initial background is assigned to a peak, the background spectrum is multiplied by a constant and subtracted from the sample spectrum when the peak is coadded. The peak table is automatically updated for each edit made in the chromatograms.

From the absorbance mode display, the absorbance spectrum of individual peaks or scan-sets are zoomed and rolled for a close examination.

From the peak table mode, detailed peak information is given.

GC Coadd

The GC coadd commands absorbance spectra for every peak in the peak table. (From the peak editor, absorbance spectra can be coadded for defined peaks.) The GC compute command takes the peak table as input and coadds the selected peak absorbance scan-sets. If a background region other than the initial background spectrum is assigned to the peak, the GC coaddition autosubtract algorithm is used to compensate for interfering substances.

(Sample peak) - (background spectrum) * (Subtraction factor)

The background spectrum is multiplied by a factor to accurately compensate for the species being subtracted, then is subtracted from the sample peak.

Peak print

Same as that of non-array processor.

Save run

Same as that of non-array processor.

Spectral search

Same as that of non-array processor.

Plotting Spectra and GSC

Same as that of non-array processor.

REFERENCES

1 Kreisher, K.R. "PVC is a Good Bet to Survive its Global Environmental Travail." Modern Plastics (MPT), June, 67 (1990): 60-64.

2 Ushida, S., Kamo, H., Kubota, H, and Kanaya, K. "Reaction Kinetics of Formation of HCl in Municipal Refuse Incinerators." *Ind. Eng. Chem. Process Des. Dev.*, 22 (1983):144.

3 Lao, Q. "The Removal of HCl from Hot Gases with Calcium Compounds." 1992 Thesis at NJIT.

4 Karlson, H.T.; Klingstor, I.; Bjerle, I. "Adsorption of Hydrochloric Acid on Solid Slaked Lime for Flue Gas Clean Up." *J. Air Pollut. Control Assoc.*, 31 (1981): 1177.

5 Walters, J.K.; Daoudi, M. The "Removal of Hydrogen Chloride from Hot Gases Using Calcined Limestone." In *Management of Hazardous and Toxic Wastes in the Process Industrial*; Kolaczkowski, S.T., Crittenden, B.D.,Eds.; Elsevir: London, 1987, pp 574-583.

6 Weinell, C.E.; Jenson, P. I.; Kim Dam-Johansen; Hans Livbjerg "Hydrogen Chloride Reaction with Lime and Limestone: Kinetics and Sorption Capacity." *Ind. Eng. Chem. Res.* 31(1992): 164.

7 Gullett, B.K.; Jozewicz, W; Stefanski, L.A. "Reaction Kinetics of Ca-Based Sorbents with HCl. *Ind. Eng. Chem. Res.*, 11 (1992): 2437-2446.

8 Daoudi, M., Dissertation for the Ph.D. Degree, The British Library Document Supply Center. West Yordshire United Kingdom, 1987.

9 Wen, C.Y. "Non-catalytic Heterogeneous Solid Fluid Reaction Model" *Ind. Eng. Chem.*, 60 (1968): 34.

10 Smith, J.M., Chemical Engineering Kinetics. 1981, McGraw Hill, 3rd edition, New York.

11 Levenspiel, O. Chemical Reaction Engineering. 1981, John Wiley and Sons, Inc., New York.

12 Gopalakrishnan, R. "A Novel Application of FT-IR Spectroscopy for the Kinetics of High-Temperature Reaction of SO_2 with CaO." *Applied Spectroscopy* 2 (1990): 310-313.

13 Ranz, W.E.; Marshall, W.R. "Evaporation from Drops" *Chem.Eng.Prog.* 48 (1952): 141-146.

14 Levenspiel, O. Chemical Reaction Engineering. 1972, Wiley, New York.